nature cell biology

USP4 is regulated by AKT phosphorylation and directly deubiquitylates TGF-β type I receptor

Long Zhang[1,6], FangFang Zhou[1,6,7], Yvette Drabsch[1], Rui Gao[2], B. Ewa Snaar-Jagalska[3], Craig Mickanin[4], Huizhe Huang[5], Kelly-Ann Sheppard[4], Jeff A. Porter[4], Chris X. Lu[4] and Peter ten Dijke[1,7]

The stability and membrane localization of the transforming growth factor-β (TGF-β) type I receptor (TβRI) determines the levels of TGF-β signalling. TβRI is targeted for ubiquitylation-mediated degradation by the SMAD7–SMURF2 complex. Here we performed a genome-wide gain-of-function screen and identified ubiquitin-specific protease (USP) 4 as a strong inducer of TGF-β signalling. USP4 was found to directly interact with TβRI and act as a deubiquitylating enzyme, thereby controlling TβRI levels at the plasma membrane. Depletion of USP4 mitigates TGF-β-induced epithelial to mesenchymal transition and metastasis. Importantly, AKT (also known as protein kinase B), which has been associated with poor prognosis in breast cancer, directly associates with and phosphorylates USP4. AKT-mediated phosphorylation relocates nuclear USP4 to the cytoplasm and membrane and is required for maintaining its protein stability. Moreover, AKT-induced breast cancer cell migration was inhibited by USP4 depletion and TβRI kinase inhibition. Our results uncover USP4 as an important determinant for crosstalk between TGF-β and AKT signalling pathways.

TGF-β is essential for embryogenesis and tissue homeostasis in multicellular organisms[1,2]. Perturbations in TGF-β signalling have been linked to a diverse set of human diseases, including cancer[3,4]. The TGF-β serine/threonine kinase receptor phosphorylates receptor-regulated (R)-SMADs, that is, SMAD2 and SMAD3. Activated R-SMADs form hetero-oligomers with SMAD4 that accumulate in the nucleus and regulate a large number of target genes[1–4]. In addition, non-SMAD signalling pathways such as phosphatidylinositol-3-OH kinase (PI(3)K)–AKT pathway are initiated[5–8]. These non-canonical pathways are also activated by tyrosine kinase receptors that mediate growth-factor-induced cell proliferation, survival and migration[9]. During cancer progression, TGF-β frequently switches from tumour suppressing to tumour promoting[3,4]. Oncogenic signals may blunt TGF-β-induced growth arrest and apoptosis, while enhancing TGF-β-induced pro-invasive and pro-metastatic responses[10–13]. This may involve a change in the balance between canonical and non-SMAD signalling[14–16].

Ubiquitin modification of TGF-β signalling components is emerging as a key mechanism of TGF-β pathway control[17,18]. Proteasomal degradation mediated by SMURF E3 ubiquitin ligase regulates the sensitivity and duration of TGF-β signalling response by regulating the abundance of R-SMADs both before and after signal initiation[19–22]. The conjugating function of E3 ligases is opposed by deubiquitylating enzymes[23–26] (DUBs). Ubiquitin-specific peptidase 15 (USP15) was identified as a deubiquitylating enzyme for R-SMADs (ref. 27). Another example is provided by SMAD7-mediated recruitment of SMURF2 to the activated TβRI, which targets this receptor for degradation[28,29]. Recently, USP15 was shown to counteract this response by binding to the SMAD7–SMURF2 complex[30]. In this study, we identified USP4 as a potent enhancer of TGF-β signalling by directly deubiquitylating TβRI, thereby maintaining sustained TβRI levels at the plasma membrane. Growth factors and TGF-β-induced AKT activation mediates USP4 phosphorylation and relocalization to the membrane, and thereby reinforces pro-tumorigenic functions induced by the TGF-β receptor in breast cancer cells.

RESULTS

USP4 is a critical component in TGF-β signalling

To identify critical regulators of TGF-β signalling, we performed a gain-of-function screen overexpressing 27,000 genes using a SMAD3-4-dependent transcriptional luciferase reporter as a readout system. Multiple DUBs, including USP4, USP15 and USP19, potently

[1]Department of Molecular Cell Biology, Leiden University Medical Center, Postbus 9600 2300 RC Leiden, The Netherlands. [2]School of Life Sciences, Xiamen University Center, Xiamen, Fujian 361005, China. [3]Institute of Biology, Leiden University, Einsteinweg 55, 2333 CC Leiden, The Netherlands. [4]Novartis Institutes for Biomedical Research, 250 Massachusetts Avenue, Cambridge, Massachusetts 02139, USA. [5]Faculty of Basic Medical Sciences, Chonqing Medical University, Medical College Road 1, 400016 Chongqing, China. [6]These authors contributed equally to this work.
[7]Correspondence should be addressed to F.Z. or P.t.D. (e-mail: F.zhou@lumc.nl or p.ten_dijke@lumc.nl)

Received 20 January 2012; accepted 11 May 2012; published online 17 June 2012; DOI: 10.1038/ncb2522

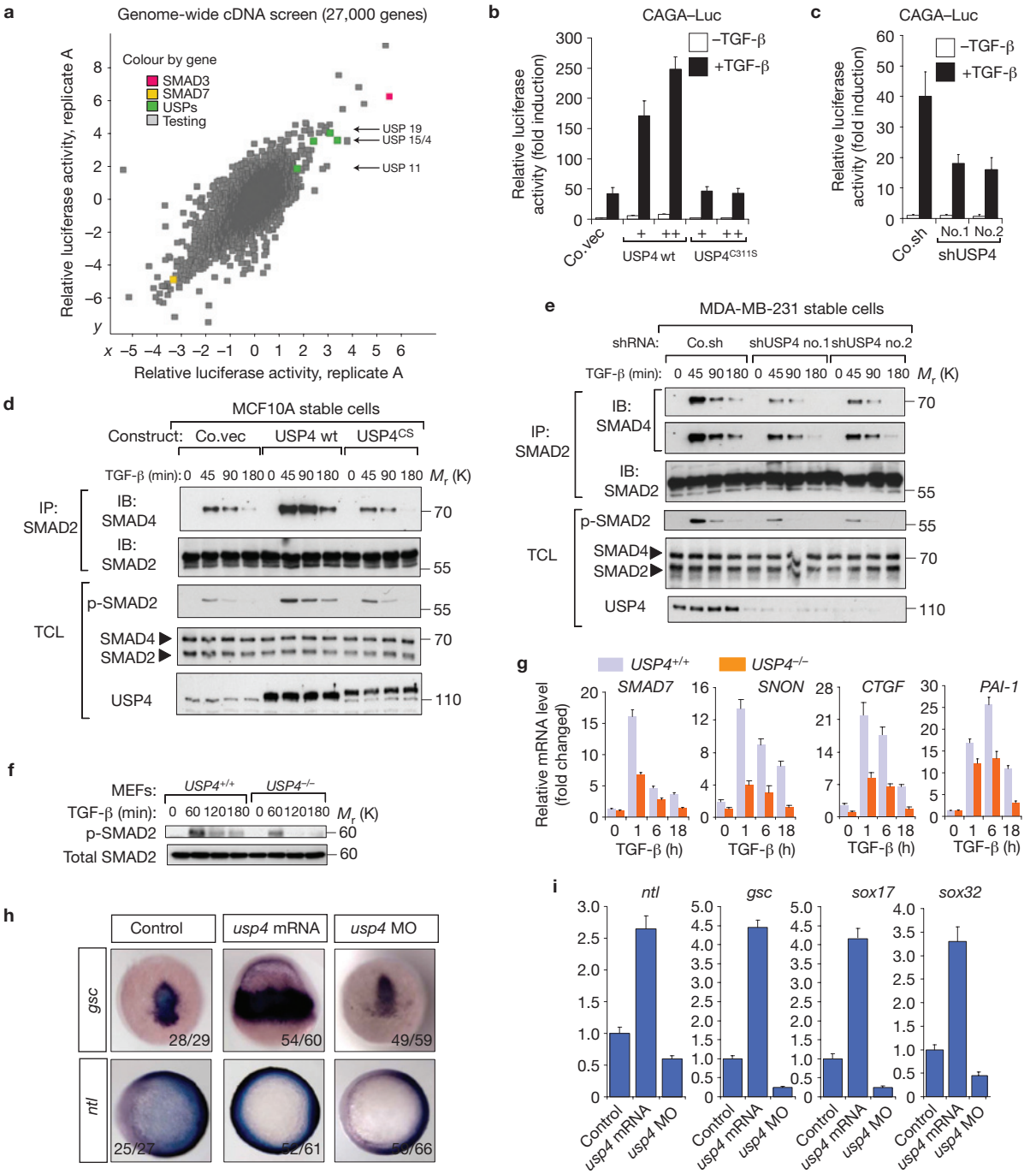

Figure 1 USP4 is a DUB required for TGF-β signalling. (**a**) Diagram of genome-wide cDNA screening data in HEK293T cells in which USPs that activate the TGF-β-induced SMAD3–SMAD4-dependent $CAGA_{12}$–Luc transcriptional reporter are indicated. Testing refers to individual cDNAs that were analysed. The *x* and *y* axes are the relative luciferase activity in two replicates, $P < 0.01$. (**b**,**c**) Effect of USP4 wt and the USP4 deubiquitin enzyme activity inactive mutant ($USP4^{CS}$). (**b**) or knockdown (shUSP4 no. 1 and no. 2) (**c**) on $CAGA_{12}$–Luc transcriptional response induced by TGF-β (5 ng ml^{-1}) in HEK293T cells. Data are presented as means ±s.d. Co.vec, empty vector; Co.sh, non-targeting shRNA. (**d**,**e**) Immunoprecipitation (IP) and immunoblot (IB) analysis of SMAD2–SMAD4 complex formation in MCF10A-Ras breast epithelial cells on overexpression of USP4 wt or $USP4^{CS}$ (**d**) or on knockdown of USP4 by shRNA (shUSP4 no. 1 and no. 2) (**e**) and stimulated with TGF-β (5 ng ml^{-1}) for the indicated times. (**f**) Kinetics of TGF-β (5 ng ml^{-1})-induced SMAD2 phosphorylation in wt MEFs (*USP4* wt) and USP4 knockout MEFs ($USP4^{-/-}$). Cell lysates were immunoblotted for phosphorylated SMAD2 (p-SMAD2) and total SMAD2. (**g**) qRT-PCR analysis of TGF-β target genes *SMAD7*, *SnoN*, *CTGF*, *and PAI-1* in *USP4* wt and *USP4* deficient MEFs treated with TGF-β (5 ng ml^{-1}) for the indicated times. Values and error bars represent the means ±s.d. of triplicates and are representative of at least two independent experiments. (**h**) The expression patterns of *no tail* (*ntl*) and *goosecoid* (*gsc*) under conditions of *usp4* overexpression (*usp4* mRNA, 100 ng) or knockdown (*usp4* morpholino (MO), 0.5 ng). All embryos are shown in the 70% epiboly stage. The numbers of observed embryos are shown. All of the embryo injections were carefully controlled with the same amount of control morpholino and control GFP mRNA. (**i**) qRT-PCR analysis of zebrafish embryos with *usp4* overexpression (*usp4 mRNA*) or knockdown (*usp4* MO). Values and error bars represent the means ±s.d. of triplicates and are representative of at least two independent experiments. Uncropped images of blots are shown in Supplementary Fig. S8.

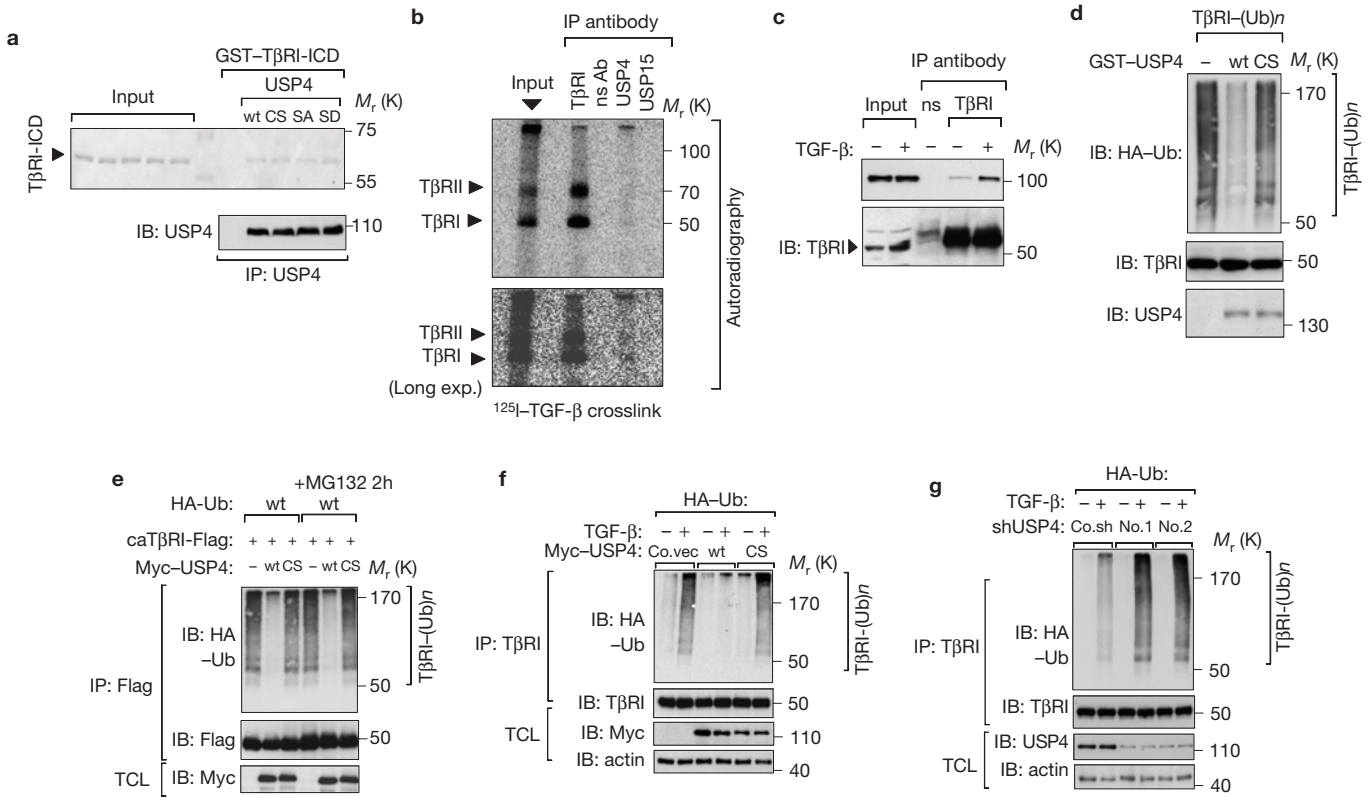

Figure 2 USP4 interacts with TβRI and deubiquitylates TβRI. (**a**) Purified USP4 wt and mutants bound to indicated GST–TβRI-ICD (intracellular domain) *in vitro*. SA, USP4^{S445A} mutant; SD, USP4^{S445D} mutant. (**b**) Endogenous TGF-β receptors of MDA-MB-231 cells were covalently affinity labelled with ^{125}I-labelled TGF-β ligand; cell lysates were then collected for immunoprecipitation with TβRI, non-specific (ns), USP4 or USP15 antibodies as indicated. Endogenous TβRI and TβRII that were immunoprecipitated by antibodies were detected by autoradiography. (**c**) TGF-β treatment increased the endogenous interaction between USP4 and TβRI as demonstrated by immunoprecipitation and immunoblot analysis of MDA-MB-231 cells treated with TGF-β (5 ng ml^{-1}) for 4 h. Input and immunoprecipitation with non-specific (ns) and TβRI antibody are shown. (**d**) Poly-HA-ubiquitylated TβRI substrate (purified in denaturing conditions) was incubated with purified recombinant USP4 wt or USP4^{CS} at 37 °C for 1 h. The reaction was terminated by the addition of SDS sample buffer followed by a 2 min heat denaturation at 95 °C. Reaction products were detected by western blot analysis using the indicated antibodies. (**e**) Immunoblot analysis of whole cell lysate (TCL) and immunoprecipitates derived from HEK293T cells transfected with HA–Ub, TβRI–Flag, and Myc–USP4 wt or USP4^{CS} and treated with or without MG132 for 2 h as indicated. caTβRI, constitutively active TβRI. (**f**) HA–Ub-expressing HEK293T cells were transfected with Myc–USP4 wt or USP4^{CS} and treated with TGF-β (5 ng ml^{-1}) for 2 h as indicated. Cells were then collected for immunoprecipitation with anti-TβRI antibody followed with immunoblot analysis. (**g**) HA–Ub expressed HEK293T cells were infected with control (Co.vec) and two independent lentivirus-mediated USP4 shRNA (no. 1 and no. 2) and treated with TGF-β (5 ng ml^{-1}) for 2 h as indicated. Cells were collected for immunoprecipitation with TβRI antibody followed with immunoblot analysis. Uncropped images of blots are shown in Supplementary Fig. S8.

activated the TGF-β-induced signal (Fig. 1a). Independent screens with 69 Flag-tagged DUB complementary DNAs using SMAD-dependent and other pathway reporter assays confirmed these USPs as selective activators of TGF-β (Supplementary Fig. S1a and Table S1; ref. 31).

As USP4 was the strongest DUB for TGF-β activation, we investigated its role in TGF-β signalling in detail. USP4^{CS} (carrying a point mutation in one of the key cysteines of the catalytic domain) did not potentiate TGF-β signalling (Fig. 1b), suggesting that DUB activity is essential. Knockdown assays demonstrated that USP4 is required for a proper TGF-β-induced transcriptional response (Fig. 1c). Ectopic expression of USP4 wild type (wt), but not USP4^{CS}, increased the magnitude and duration of TGF-β-induced SMAD2 phosphorylation and SMAD2–SMAD4 complex formation in MCF10A-Ras breast cancer cells (Fig. 1d). Depletion of USP4 had the opposite effect in MDA-MB-231 breast cancer cells (Fig. 1e). Moreover, TGF-β-induced SMAD2 phosphorylation and target gene expression were impaired in USP4-deficient mouse embryonic fibroblasts (MEFs; Fig. 1f,g).

To investigate the role of USP4 *in vivo*, we depleted *usp4* in zebrafish using morpholino oligonucleotides (with depleting effects confirmed) and observed a serious epiboly defect before the formation of the tail bud is completed (data not shown). Moreover, transcriptional reporter assays in zebrafish embryos showed that *usp4* misexpression has a strong effect on TGF-β—but not on BMP signalling (Supplementary Fig. S1b,c). Consistently, *in situ* hybridization showed that *usp4* morphant embryos express only low amounts of the TGF-β signalling targets *goosecoid (gsc)* and *notail (ntl)*, whereas these genes were upregulated in embryos injected with *usp4* messenger RNA (Fig. 1h). Quantitative real-time PCR (qRT-PCR) analysis of *gsc*, *ntl*, *sox17* and *sox32* confirmed the effects of USP4 misexpression on TGF-β target genes (Fig. 1i). Taken together, these results indicate that USP4 is a critical and selective regulator of TGF-β signalling in mammalian cells and zebrafish embryos.

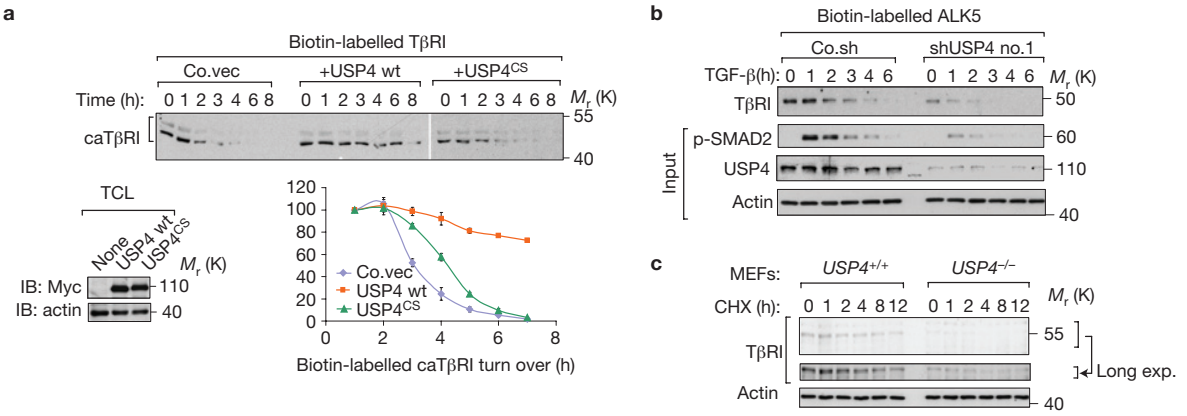

Figure 3 USP4 stabilizes membrane receptor levels of TβRI. (**a**) Biotinylation analysis of cell surface receptors. COS7 cells transfected with constitutively active (ca) TβRI–Flag along with or without USP4 wt or USP4^{CS} were biotinylated for 40 min at 4 °C and then incubated at 37 °C for various times. The biotinylated cell surface receptors were precipitated with streptavidin beads and analysed by anti-Flag immunoblotting. Lower right panel: quantification of the band intensities in the upper panel. Band intensity was normalized to the $t = 0$ controls. Results are shown as means ±s.d. of three independent sets of experiments. (**b**) MDA-MB-231 cells infected with control (Co.sh) or USP4 shRNA lentivirus (no. 1) were biotinylated for 40 min at 4 °C and then incubated at 37 °C with TGF-β (5 ng ml^{-1}) for the indicated times to stimulate receptor internalization and treated with TGF-β (5 ng ml^{-1}) for different times as indicated. The biotinylated cell surface receptors were precipitated with streptavidin beads and analysed by anti-TβRI immunoblotting. Whole cell lysates (5%) were loaded as inputs showing p-SMAD2 and USP4 levels. Actin was included as a loading control. (**c**) Expression levels of TβRI were analysed by immunoblot analysis in *USP4* wt and *USP4* deficient MEFs treated with cyclohexamide (CHX, 20 μg ml^{-1}) for the indicated times. Immunoblotting for actin was included as a reference. Uncropped images of blots are shown in Supplementary Fig. S8.

USP4 directly interacts with and deubiquitylates TβRI

The results above indicate that USP4 acts as a TGF-β pathway deubiquitylase upstream of R-SMAD activation. We therefore investigated whether USP4 targets the TGF-β receptor. *In vitro* the TβRI intracellular domain was found to associate directly with USP4 (Fig. 2a). On overexpression, USP4 bound TβRI through its carboxy-terminal USP domain (Supplementary Fig. S2a and and data not shown). Importantly, the binding of (endogenous) USP4 was more efficient on TβRI activation (Supplementary Fig. S2a,b). On ectopic expression of USP4 and TβRI, USP4 co-localized with activated TβRI in the cytosol and in the plasma membrane (Supplementary Fig. S2c,d). Moreover, USP4 antibodies co-immunoprecipitated ^{125}I–TGF-β affinity-labelled endogenous receptors (Fig. 2b). Furthermore, endogenous USP4 was found to interact with TβRI in a TGF-β-induced manner in HeLa cells (Fig. 2c). Thus, USP4 binds TβRI at physiological conditions.

Next we investigated whether USP4 affects TβRI ubiquitylation. The TβRI-associated USP4 wt was not ubiquitylated, but the TβRI-associated USP4^{CS} mutant was highly ubiquitylated (Supplementary Fig. S2e). We therefore examined whether USP4 serves as a DUB for TβRI. First, Flag-tagged constitutively active TβRI proteins were affinity purified, and their ubiquitylation pattern was visualized by immunoblotting for HA–ubiquitin: polyubiquitylation appeared as a major modification of TβRI. To demonstrate that USP4 can directly deubiquitylate TβRI we performed *in vitro* deubiquitylation assays. Purified glutathione *S*-transferease (GST)–USP4 wt, but not GST-USP4^{CS}, removed polyubiquitin chains from TβRI (Fig. 2d). Overexpression of USP4 wt, but not USP4^{CS}, inhibited TβRI polyubiquitylation in the absence or presence of the proteasome inhibitor MG132 (Fig. 2e).

TGF-β receptor signalling induces SMAD7 expression, which subsequently mediates TβRI degradation by recruiting the E3 ligase SMURF2 (refs 28,29). USP4 opposed SMAD7–SMURF2-induced TβRI ubiquitylation (Supplementary Fig. S2f) and blocked TGF-β-induced TβRI ubiquitylation at the endogenous level (Fig. 2f). Conversely, USP4 depletion enhanced TGF-β-induced TβRI polyubiquitylation (Fig. 2g). Polyubiquitylation of TβRI has been reported to promote its internalization and degradation[32]. We therefore investigated whether USP4 misexpression affects TβRI levels at the plasma membrane, where signalling is initiated[32]. Biotin-labelled cell surface TβRI displayed a prolonged half-life on co-expression with USP wt, but not with USP4^{CS} (Fig. 3a). In line with this, USP4 depletion in MDA-MB-231 cells led to lower cell surface TβRI levels and accelerated degradation (Fig. 3b). Moreover, USP4-deficient MEFs showed lower expression levels and shorter half-lives of TβRI than USP4 wt MEFs (Fig. 3c). These findings indicate that USP4 is a DUB for TβRI and contributes to the increased stability of TβRI at the plasma membrane.

USP4 promotes TGF-β-induced EMT, invasion and metastasis

USP4 is highly expressed in various cancers[33], including breast cancer (Supplementary Fig. S3a). TGF-β stimulates epithelial-to-mesenchymal transition (EMT), migration, invasion and metastasis of breast cancer cells[34]. Typical EMT characteristics include: upregulation of N-cadherin, fibronectin, smooth muscle actin and vimentin, and down-regulation of E-cadherin[35]. On depletion of USP4, TGF-β-induced changes in EMT-marker expression were attenuated (Fig. 4a), whereas ectopic expression of USP4 wt, but not USP4^{CS}, had the reverse effect (Fig. 4b). USP4 knockdown also attenuated TGF-β-induced migration of MDA-MB-231 cells (Fig. 4c). Thus, USP4 can regulate TGF-β-induced EMT and migration of breast cancer cells *in vitro*.

We next examined the effect of USP4 misexpression in breast cancer cells *in vivo* using a zebrafish embryo xenograft invasion–metastasis model[36]. MCF10A-Ras cells (which show intermediate aggressive behaviour) were injected into the zebrafish embryonic blood circulation

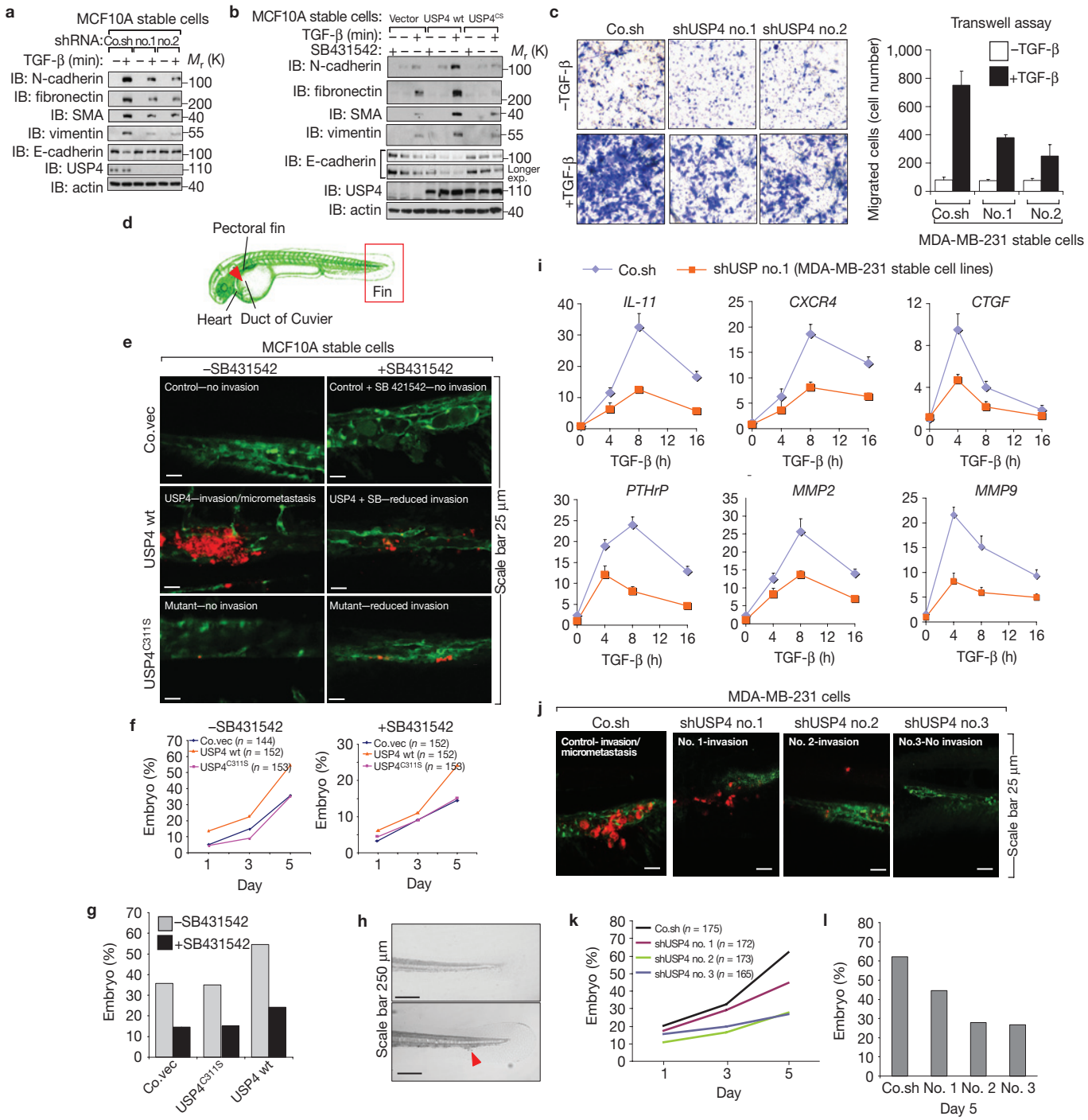

Figure 4 USP4 increases TGF-β-induced EMT, invasion and metastasis. (**a**,**b**) Immunoblot analysis of control and USP4 stably depleted (with shRNA no. 1 or no. 2) (**a**) or USP4 wt or USP4^{CS} stably expressed (**b**) MCF10A-Ras cells treated with TGF-β (5 ng ml^{-1}) and SB431542 (5 μM) for 36 h as indicated. (**c**) USP4 depletion inhibits TGF-β-induced migration. Migrated cells were counted from four random fields, and means ±s.d. were calculated ($P < 0.05$). Representative results are shown in the left panel. (**d**) Schematic diagram of zebrafish embryo. (**e**) MCF10A-Ras cells stably expressing control vector (Co.vec), USP4 wt or USP4^{CS} were injected into the blood circulation of 48-hpf zebrafish embryos. Cells were treated with or without SB431542 (10 μM) for 24 h before injection, and SB431542 (5 μM) was added to the zebrafish environment. Representative images of zebrafish at 5 dpi are shown. (**f**) Percentage of embryos exhibiting invasion are shown at 1, 3 and 5 dpi. (**g**) The final percentage of zebrafish embryos exhibiting invasion at 5 dpi. The results of two independent experiments are shown. (**h**) Representative light microscopy image of the posterior tail of a control zebrafish embryo (upper panel) and a 5-dpi zebrafish embryo exhibiting invasion of MCF10A-Ras cells (lower panel). The red arrow indicates metastatic cells. (**i**) qRT-PCR analysis of TGF-β target and invasion-related genes in MDA-MB-231 cells infected with non-targeting shRNA (Co.sh) or USP4 shRNA (shUSP4 no. 1) and treated with TGF-β (5 ng ml−1) for the indicated times. $n = 3$. (**j**–**l**) MDA-MB-231 cells stably infected with empty vector (Co.sh) or three independent USP4 shRNAs (no. 1, no. 2, and no. 3) were injected into the blood circulation of 48-hpf zebrafish. Representative images of zebrafish at 5 dpi are shown (**j**). Invasion (**k**) and experimental micrometastasis (**l**) were detected in the posterior tail fin over 5 days. The final percentage of embryos exhibiting metastasis at 5 dpi is shown. The results of two independent experiments are shown ($P < 0.05$). Uncropped images of blots are shown in Supplementary Fig. S8.

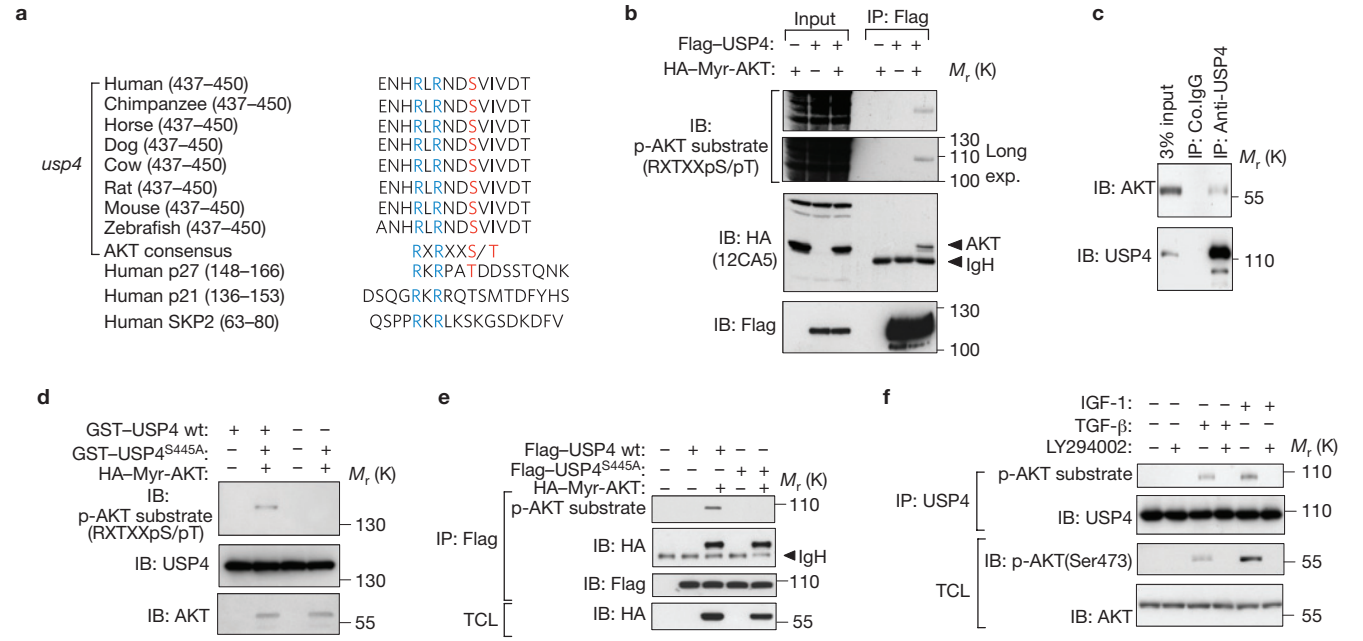

Figure 5 AKT phosphorylates USP4. (**a**) Sequence alignment of the AKT phosphorylation site within USP4 orthologues of different species and known AKT substrates p27, p21 and Skp2. (**b**) AKT interacts with and phosphorylates USP4. HEK293T cells were transfected with indicated plasmids and collected for co-immunoprecipitation and immunoblot analysis. (**c**) Endogenous interaction between USP4 and AKT detected in HeLa cells. Cell lysates were subjected to immunoprecipitation with USP4 antibody followed by immunoblotting with AKT antibody. (**d**) AKT phosphorylates USP4 *in vitro* at Ser 445. HA–Myr-AKT was transfected into 293T cells, recovered by anti-HA immunoprecipitation and incubated with 5 μg of the indicated GST–USP4 in the presence of unlabelled ATP. The kinase reaction products were resolved by SDS–PAGE, and phosphorylation was detected by the phospho-AKT substrate antibody that recognizes either the RXRXXpS(pT) or the R-KXR-KXXpS(pT) motif. (**e**) AKT phosphorylates USP4 *in vivo*. Immunoblot analysis of whole cell lysate and immunoprecipitates derived from HEK293T cells transfected with Flag–USP4 wt, Flag–USP4 S445A, and/or HA–Myr-AKT1 plasmids. (**f**) Immunoblot analysis of TCL and immunoprecipitates derived from serum-starved HeLa cells treated with IGF-1 (200 ng ml^{-1}), TGF-β (5 ng ml−1) and LY294002 (50 μM) for 8 h as indicated. Uncropped images of blots are shown in Supplementary Fig. S8.

(Fig. 4d). After 5 days, a marked increase in MCF10A-Ras cell invasion was visible on ectopic expression of USP4 wt, but not of USP4^{CS} (Fig. 4e,f). Treatment with SB431542, a selective TβRI kinase inhibitor, reduced the invasion and micrometastasis of all samples (Fig. 4f,g). After 5 days, USP4 wt expression in MCF10A-Ras cells resulted in 55% of embryos exhibiting invasion, whereas the USP4^{CS} and control cells showed invasion in 35% and 36% embryos, respectively ($P < 0.01$; Fig. 4f,g). Owing to the transparent nature of the embryo, invading cells were also visible with light microscopy (Fig. 4h).

MDA-MB-231 is a highly aggressive human breast cancer cell line, and metastasis of these cells in a mouse xenograft model was found to be dependent on TGF-β receptor signalling in tumour cells[37,38]. qRT-PCR analysis of MDA-MB-231 cells with short hairpin (sh)RNA-mediated USP4 knockdown indicated that endogenous USP4 is required for efficient induction of metastasis-related TGF-β target genes, such as *IL-11*, *CTGF*, *CXCR4*, *PTHrP* and *MMPs* (Fig. 4i).

To examine their invasion and metastasis properties in zebrafish embryos, USP4-depleted MDA-MB-231 cells were injected into the ducts of Cuvier 48 hours post-fertilization (hpf) and analysed over 5 days post-injection (dpi; see representative images of the tail fin area in Fig. 4j). Sixty-two per cent of embryos showed invasion in the case of control cells, whereas knockdown of USP4 by three independent shRNAs significantly reduced this amount (Fig. 4k). The amount of micrometastasis was also reduced on USP4 depletion (Fig. 4l). Taken together, these results suggest that USP4 stimulates TGF-β-induced breast cancer invasion and metastasis. Of note, we found that overexpression of USP4 potentiates the TGF-β-induced cytostatic effects in HaCaT keratinocytes (Supplementary Fig. S3b and data not shown): in contrast to many (breast) cancer cells the USP4 levels are low in HaCaT cells (Supplementary Fig. S3c) and USP4-mediated enhancement of the growth inhibitory effects by TGF-β may not be physiologically relevant.

AKT phosphorylates USP4 and redirects its subcellular localization

As previously mentioned, ectopically expressed USP4 and activated TβRI co-localized in the cytosol and plasma membrane on TGF-β treatment. However, when we analysed the subcellular distribution of endogenous USP4 (which contains nuclear localization and export sequence motifs), we detected it mainly in the nucleus. This prompted us to investigate how USP4 could regulate cell surface TβRI levels at the plasma membrane. Sequence analysis revealed that USP4 contains an AKT consensus RxRxxS(T) phosphorylation motif[39] at Ser 445, which is conserved in USP4 orthologues (Fig. 5a). Phosphorylation of certain AKT substrates controls their nuclear accumulation[40]. We therefore reasoned that AKT might phosphorylate USP4 and thereby influence its subcellular localization. Consistent with this hypothesis, we found that an activated allele of AKT (Myr-AKT1) interacts with USP4 in transfected cells (Fig. 5b). In addition, USP4 was found to associate with AKT both *in vitro* and *in vivo* (Fig. 5c and Supplementary Fig. S4a). To examine whether USP4 indeed is a substrate for AKT, we used a phospho-specific antibody that recognizes the optimal AKT phosphorylation consensus motif. This p-AKT substrate antibody showed that activated AKT significantly

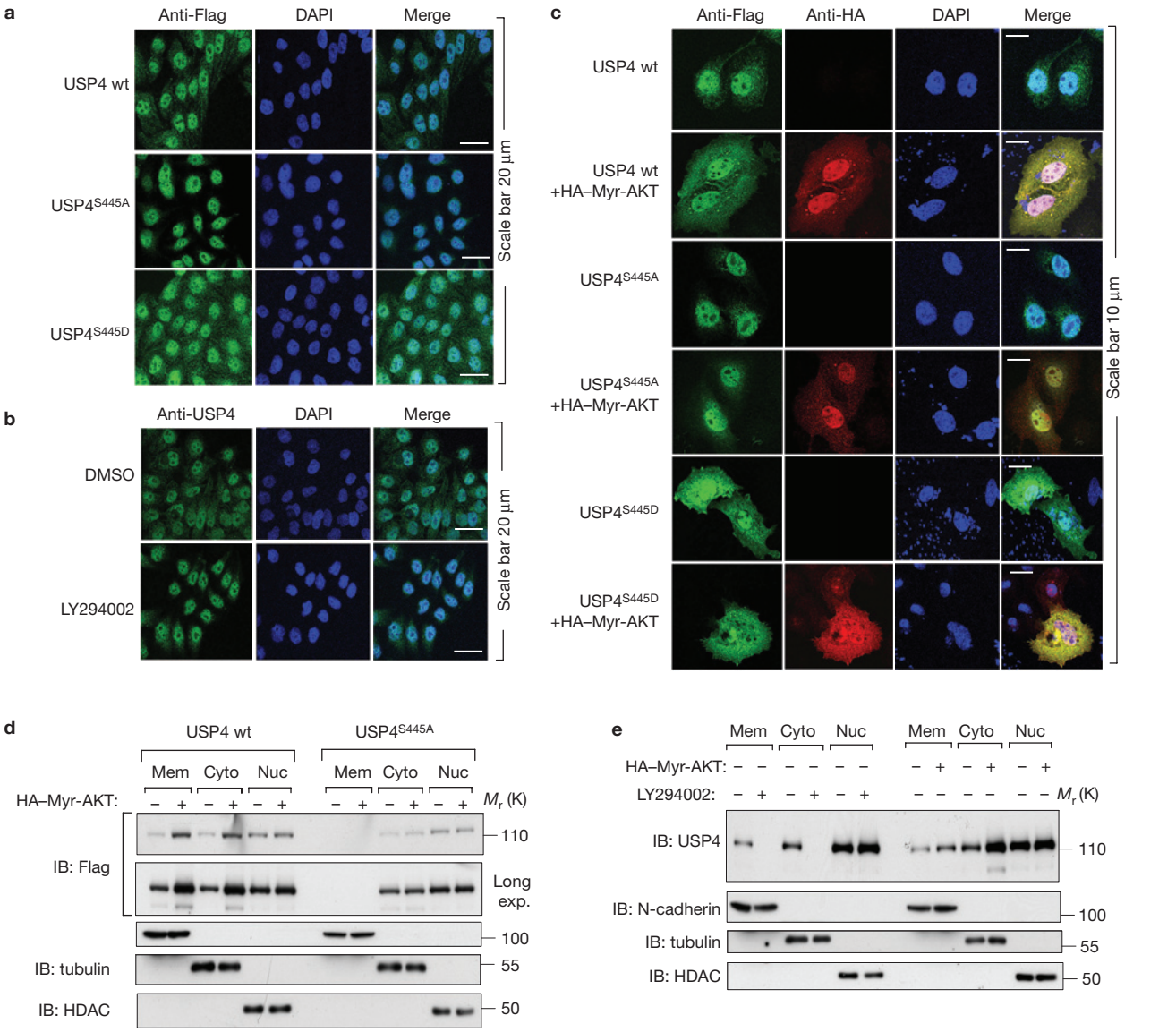

Figure 6 AKT activation promotes the membrane and cytoplasmic localization of USP4. (**a**) Immunofluorescence and 4,6-diamidino-2-phenylindole (DAPI) staining of HeLa cells stably transfected with USP4 WT, S445A or S445D plasmids. (**b**) Immunofluorescence and DAPI staining of HeLa cells treated with control (dimethylsulphoxide; DMSO) or LY294002 (50 μM) for 8 h. (**c**) Immunofluorescence and DAPI staining of HeLa cells transfected with HA–Myr-AKT along with USP4 wt, USP4^{S445A} or USP4^{S445D}. (**d**) HeLa cells transfected with USP4 wt, USP4^{S445A} and HA–Myr-AKT as indicated were collected for membrane, cytoplasm and nuclear extraction, followed by immunoblot analysis. (**e**) HeLa cells were transfected with HA–Myr-AKT. Thirty hours after transfection, cells were treated with LY294002 (50 μM) for 8 h as indicated. Cells were then collected for membrane, cytoplasm and nuclear extraction, followed by immunoblot analysis. For **d**,**e** N-cadherin, tubulin and histone deacetylase (HDAC)3 were analysed as the membrane (mem), cytoplasm (cyto) and nuclear (nuc) fraction markers, respectively. Uncropped images of blots are shown in Supplementary Fig. S8.

stimulated the phosphorylation of USP4 wt both *in vitro* and *in vivo*, whereas phosphorylation of USP4^{S445A} was not detected (Fig. 5b,d,e and Supplementary Fig. S4b). The reactivity of USP4 with this antibody was reversed when the cell lysates were incubated with lambda phosphatase (Supplementary Fig. S4c). Both insulin-like growth factor (IGF)-1- and TGF-β-induced phosphorylation of endogenous USP4 was detected by the AKT substrate antibody. Notably, the level of phosphorylation of USP4 was decreased in cells that were treated with LY294002, a selective inhibitor of PI(3)K (Fig. 5f).

To investigate the effect of AKT on USP4 subcellular localization, we performed confocal analysis in HeLa cells stably expressing USP4 wt or USP4 S445A (S445D) mutants. These Ser 445 mutations do not affect DUB activity and the ability to interact with TβRI *in vitro* (Fig. 2a and Supplementary Fig. S7g,h). Whereas USP4^{S445A} was almost exclusively present in the nuclei, USP4^{S445D} showed a significant increase in cytoplasmic localization when compared with USP4 wt (Fig. 6a and Supplementary Fig. S4d). Importantly, LY294002 treatment reduced the cytoplasmic signal of endogenous USP4 (Fig. 6b). To validate these findings, we examined the effect of activated Myr-AKT on the localization of USP4 wt or USP4 S445A (S445D) using immunofluorescence microscopy and cellular fractionation. Expression of activated Myr-AKT promoted the cytoplasmic and membrane localization of USP4 wt (Fig. 6c,d). In contrast, USP4^{S445A} was still restricted to the nuclear compartment in the presence of

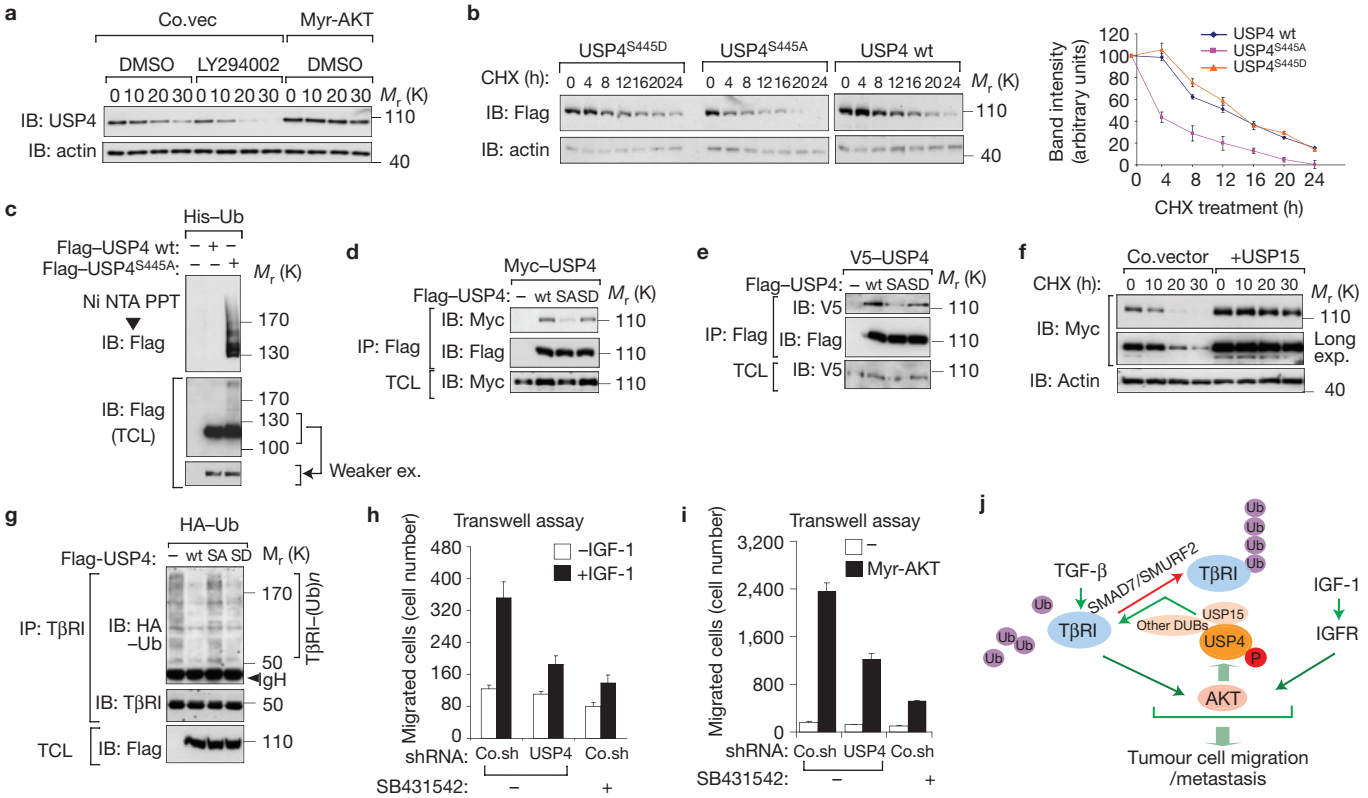

Figure 7 AKT-mediated phosphorylation affects USP4 stability and DUB activity towards TβRI. (**a**) Immunoblot analysis of HeLa cells transfected with empty vector (Co.vec) or Myr-AKT and treated with DMSO, LY294002 (50 μM) and CHX (20 μg ml^{-1}) as indicated. Actin was included as a loading control. (**b**) Left panel: Immunoblot analysis of HEK293T cells transfected with USP4^{S445D}, USP4^{S445A} or USP4 wt and treated with CHX (20 μg ml^{-1}) for the indicated times. Right panel: Quantification of the band intensities in the left panel. Band intensity was normalized to the $t = 0$ controls. Results are shown as means ±s.d. of three independent sets of experiments. (**c**) HEK293T cells stably expressing His–Ub were transfected with Flag–USP4 wt or the Flag–USP4^{S445A} mutant and collected for Ni NTA pulldown and immunoblot analysis. (**d**,**e**) Immunoblot analysis of whole cell lysate and immunoprecipitates derived from HEK293T cells transfected with Myc–USP4 (**d**) or V5–USP15 (**e**) along with Flag-USP4 wt, USP4^{S445A} (SA), USP4^{S445D} (SD). (**f**) Immunoblot analysis of Myc–USP4-expressing HEK293T cells transfected with control empty vector (Co.vec) or USP15 and treated with CHX (20 μg ml^{-1}) for the indicated times. (**g**) Immunoblot analysis of whole cell lysate and immunoprecipitates derived from HA–Ub-expressing HEK293T cells transfected with Flag–USP4 wt, USP4^{S445A} (SA) or USP4^{S445D} (SD). (**h**) Control (Co.sh) and USP4 stably depleted MDA-MB-231 cells were plated for cell migration assays. Cells were treated with or without SB431542 (10 μM) and IGF-1 for 8 h. (**i**) Control and USP4 stably depleted MDA-MB-231 cells were infected with or without Myr-AKT and plated for cell migration assay. Cells were treated with or without SB431542 (10 μM) for 8 h. For **h** and **i**, migrated cells were counted from four random fields, and means ± s.d. were calculated ($P < 0.05$). $n = 3$. (**j**) Working model for the involvement of USP4 in the regulation of TGF-β signalling in tumour cell migration and metastasis: USP4 deubiquitylates the TβRI and is regulated by AKT-mediated phosphorylation. Uncropped images of blots are shown in Supplementary Fig. S8.

activated AKT (Fig. 6c,d). Conversely, a significant fraction of the phospho-mimetic USP4^{S445D} was located in the cytoplasm, and its localization was not affected much by the expression of activated AKT (Fig. 6c, Supplementary Fig. S4d and data not shown). Furthermore, on LY294002 treatment or activated AKT expression, the endogenous USP4 located in the membrane and cytoplasm became completely nuclear or increased in membrane and cytoplasm localization, respectively (Fig. 6e). Similarly, TGF-β could also shift USP4 to a more membrane and cytoplasmic localization (Supplementary Fig. S4e). These results together indicate that AKT-induced USP4 phosphorylation affects its subcellular distribution by promoting the presence of more USP4 in membrane and cytoplasm.

14-3-3 proteins can bind to certain AKT-phosphorylated substrates and export them from the nucleus to the cytoplasm or can retain such phosphorylated proteins in the cytoplasm[41]. Consistent with this notion, we observed that USP4 (wt and S445D, but not S445A) specifically interacted with certain 14-3-3 isoforms as purified proteins *in vitro* and in transfected cells (Supplementary Fig. S5a–e). Moreover, this interaction could be enhanced by active AKT and suppressed by LY294002 treatment (Supplementary Fig. S5e,f).

To further validate the role of AKT in the recruitment of USP4 to TβRI, we analysed the order of occurrence of TGF-β responses. USP4–AKT and USP4–TβRI interactions were immediately increased after TGF-β-induced AKT activation (pAKT Ser 473), which peaks later than phosphorylation of SMAD2. Endogenous nuclear USP4 was relocated more in the membrane and cytosol fraction after TGF-β-induced AKT activation. Basal levels of all these signalling events were reduced by treatment with LY294002 (Supplementary Fig. S6a). Moreover, when we examined the stability of TβRI at the plasma membrane in the absence or presence of LY294002 (which inhibits PI(3)K, the upstream activator of AKT), we observed that inhibition of AKT destabilized membrane TβRI (Supplementary Fig. S6b). The timing of events and requirement for PI(3)K–AKT signalling are consistent with the notion that TGF-β enhances USP4–TβRI interaction by translocating USP4 to the membrane through AKT-induced phosphorylation.

AKT-mediated phosphorylation affects USP4 stability and DUB activity

USP4 is a stable protein because it can deubiquitylate itself[42]. In line with this, USP4 wt was found to be more stable than $USP4^{CS}$ (data not shown). On inhibition or overactivation of AKT, the USP4 half-life was shortened or prolonged, respectively (Fig. 7a). Consistent with these findings, $USP4^{S445A}$ was degraded more rapidly than USP4 wt and $USP4^{S445D}$ (Fig. 7b). When compared with USP4 wt, $USP4^{S445A}$ demonstrated an increased level of conjugation with polyubiquitin chains (Fig. 7c), suggesting that the impaired protein half-life of $USP4^{S445A}$ is due to elevated ubiquitylation.

Certain DUBs can self-associate and interact with other DUBs (ref. 43). We found that USP4 could bind to itself and also interact with USP15, USP19 and USP11, the other DUBs identified in our genetic screen (Supplementary Fig. S7a). Mutation of the AKT phosphorylation site in USP4 (S445A) mitigated its ability to associate with itself or other USPs (Fig. 7d,e and Supplementary Fig. S7b). In particular, when USP4 was co-expressed with USP15, we observed an elevation in USP4 levels (Supplementary Fig. S7a) and enhanced stability of USP4 was detected (Fig. 7f). These data suggest that AKT-mediated phosphorylation on Ser 445 is required for USP4 to form homomeric complexes and heteromeric complexes with other DUBs, particularly with USP15. Intriguingly, USP4 binding partners USP15, USP19 and USP11 were also observed to deubiquitylate TβRI when they were overexpressed (Supplementary Fig. S7c). We focused on USP15 and found that it could also serve as a deubiquitylase for TβRI (Supplementary Fig. S7d). However, this USP15-mediated response relied on the presence of endogenous USP4 (Supplementary Fig. S7e).

Consistent with the notion that USP4 wt and $USP4^{S445D}$ are more abundantly located at the plasma membrane and more efficient in interacting with membrane-associated TβRI than $USP4^{S445A}$ (Supplementary Fig. S7f), we found that the $USP4^{S445A}$ mutant was unable to remove polyubiquitin chains from TβRI (Fig. 7g). This is not caused by an inactivation of DUB activity (the purified recombinant $USP4^{S445A}$ mutant was as efficient as USP4 wt in deubiquitylating Ub–AMC (Supplementary Fig. S7g) and polyubiquitylated TβRI *in vitro* (Supplementary Fig. S7h)), nor by the inability of $USP4^{S445A}$ to bind to TβRI ($USP4^{S445A}$ was as efficient as USP4 wt in TβRI interaction *in vitro* (Fig. 2a)). The reason seems to be the mislocalization of $USP4^{S445A}$: AKT-mediated USP4 phosphorylation is required for USP4 to relocate at the plasma membrane and associate with and deubiquitylate TβRI.

We showed that TGF-β-induced migration of MDA-MB-231 cells is inhibited by USP4 knockdown (Fig. 4c). This response was also inhibited by LY294002, an inhibitor of PI(3)K–AKT signalling (Supplementary Fig. S7i), which is in line with previous reports that support a role for PI(3)K–AKT signalling in TGF-β-induced migration and EMT (refs 5–8). To further investigate the role of USP4 or TGF-β signalling in IGF–AKT signalling, we examined the effect of USP4 depletion or TβRI kinase inhibition on IGF-1- or activated Myr-AKT-induced migration of MDA-MB-231 cells. We found that both treatments could reduce IGF-1–Myr-AKT-induced cell migration (Fig. 7h,i), indicating a role for both USP4 and TGF-β signalling in this response.

DISCUSSION

Here, we identified USP4 as a strong potentiator of TGF-β signalling, and showed that it deubiquitylates and stabilizes TβRI in the plasma membrane. Moreover, we found that AKT phosphorylates USP4, which induces its relocalization from the nucleus to the membrane, where it can associate with TβRI. In addition, this phosphorylation increases the stability of USP4, by promoting complex formation with itself and USP15, 11 and 19. When overexpressed, these other DUBs were also found to enhance TGF-β signalling.

A previous study ascribed a potential oncogenic function for USP4 through inhibition of p53 through ARF–BB1 and high expression in several types of human cancer[33]. Aberrant AKT activation, as a result of oncogenic mutations or excessive growth factors, occurs in many tumour cells and contributes to their survival, proliferation, migration and invasion[9]. Interestingly, high levels of TGF-β in tumours correlate with high levels of overactive PI(3)K–AKT signalling, and poor prognosis in breast cancer[5–7]. Of note, USP4 has also been shown to inhibit NF-κB signalling and to antagonize lung cancer cell migration[31,44,45], suggesting a context-dependent role for USP4 in cancer.

While this paper was under review it was reported that USP15 can deubiquitylate and stabilize TβRI (ref. 30). This is consistent with our results, although the proposed mechanism for USP15 recruitment to TβRI differs from our conclusions on USP4 (and USP15). In ref. 30, it was concluded that USP15 affects TβRI through interacting with the SMAD7–SMURF2 complex, whereas we show that USP4 acts directly on TβRI. We also found that USP15 interacts with USP4 and does not affect TβRI ubiquitylation in USP4-deficient cells. However, we did find that USP15, and not USP4, interacts with overexpressed SMAD7 (data not shown). Thus, our data suggest that USP4 enhances TβRI stabilization in a SMAD7-independent fashion and that USP15 can contribute to TβRI deubiquitylation through USP4. Importantly, in ref. 30 it was observed that USP15 is highly expressed in glioblastoma, is associated with poor prognosis and promotes TGF-β-dependent oncogenesis[30]. This parallels our results on USP4-mediated regulation of TGF-β signalling and involvement in breast cancer pathogenesis.

USP15 has also been shown to act as a DUB of monoubiquitylated R-SMADs (ref. 46). However, the authors of this study did not detect an effect of USP15 on R-SMAD phosphorylation. We could confirm that USP15 acts as a DUB of monoubiquitylated SMAD2 and SMAD3 (data not shown). Depending on the cellular context, USP15 may thus potentiate TGF-β signalling by acting at the TβRI and R-SMAD levels. Although USP4 has no DUB activity for monoubiquitylated SMAD2 and SMAD3, we do not exclude the possibility that USP4 regulates other TGF-β signalling components besides TβRI.

Our study suggests a model in which AKT activation (by growth factor or TGF-β) induces phosphorylated USP4 to relocate and stabilize TβRI in the plasma membrane, and thereby enforces TGF-β-induced pro-tumorigenic responses in breast cancer cells (Fig. 7j). It should be noted that AKT has been shown to reduce SMAD3 function in Hep3B cells in which TGF-β induces an apoptotic response[47,48]. However, SMAD3 levels are often reduced in advanced human tumours and low SMAD3 levels are sufficient for tumour promotion[49,50]. Aberrant overactivation of AKT may thus redirect TGF-β intracellular signalling and thereby contribute to its switch from tumour suppressor to tumour promoter. As DUBs can be targeted with drugs[51], it would be interesting to develop inhibitors for USP4 and examine their potential for anti-invasive and anti-metastatic roles in breast cancer cells. □

METHODS

Methods and any associated references are available in the online version of the paper at www.nature.com/naturecellbiology

Note: Supplementary Information is available on the Nature Cell Biology website

ACKNOWLEDGEMENTS

We are grateful to M. van Dinther for performing the ^{125}I–TGF-β labelling experiment, A. Teunisse and A. G. Jochemsen (Leiden University Medical Center, Leiden, The Netherlands) for 14-3-3 expression plasmids and purification of GST 14-3-3 fusion proteins, and H. van Dam for critical reading of the manuscript. We thank K. Iwata, S. Lin and S. Piccolo for reagents. This work was supported by a Netherlands Organization of Scientific Research grant (MW-NWO 918.66.606) and the Centre for Biomedical Genetics.

AUTHOR CONTRIBUTIONS

L.Z., F.Z. and P.t.D. conceived and designed the experiments; L.Z. and F.Z. carried out the biochemical and functional assays in cells. Y.D., with help from E.S.-J., performed the zebrafish assays. R.G. and H.H. conducted the zebrafish embryo assays, C.M., K-A.S. and C.X.L. performed the genome-wide gain-of-function screen and J.A.P. and C.X.L. analysed the results. L.Z., F.Z. and P.t.D. wrote the manuscript.

COMPETING FINANCIAL INTERESTS

The authors declare no competing financial interests.

Published online at www.nature.com/naturecellbiology
Reprints and permissions information is available online at www.nature.com/reprints

1. Moustakas, A. & Heldin, C. H. The regulation of TGFβ signal transduction. *Development* **136,** 3699–3714 (2009).
2. Kang, J. S., Liu, C. & Derynck, R. New regulatory mechanisms of TGF-β receptor function. *Trends Cell Biol.* **19,** 385–394 (2009).
3. Ikushima, H. & Miyazono, K. TGFβ signalling: a complex web in cancer progression. *Nat. Rev. Cancer* **10,** 415–424 (2010).
4. Massague, J. TGFβ in cancer. *Cell* **134,** 215–230 (2008).
5. Bakin, A. V., Tomlinson, A. K., Bhowmick, N. A., Moses, H. L. & Arteaga, C. L. Phosphatidylinositol 3-kinase function is required for transforming growth factor β-mediated epithelial to mesenchymal transition and cell migration. *J. Biol. Chem.* **275,** 36803–36810 (2000).
6. Muraoka, R. S. *et al.* Blockade of TGF-β inhibits mammary tumor cell viability, migration, and metastases. *J. Clin. Invest.* **109,** 1551–1559 (2002).
7. Brown, R.L. *et al.* CD44 splice isoform switching in human and mouse epithelium is essential for epithelial-mesenchymal transition and breast cancer progression. *J. Clin. Invest.* **121,** 1064–1074 (2011).
8. Lamouille, S., Connolly, E., Smyth, J. W., Akhurst, R. J. & Derynck, R. TGF-β-induced activation of mTOR complex 2 drives epithelial-mesenchymal transition and cell invasion. *J. Cell Sci.* **125,** 1259–1273 (2012).
9. Pollak, M. The insulin and insulin-like growth factor receptor family in neoplasia: an update. *Nat. Rev. Cancer* **12,** 159–169 (2012).
10. Pietenpol, J. A. *et al.* TGF-β 1 Inhibition of C-Myc transcription and growth in keratinocytes is abrogated by viral transforming proteins with pRb binding domains. *Cell* **61,** 777–785 (1990).
11. Adorno, M. *et al.* A Mutant-p53/SMAD complex opposes p63 to empower TGFβ-induced metastasis. *Cell* **137,** 87–98 (2009).
12. Oft, M. *et al.* TGF-β1 and Ha-Ras collaborate in modulating the phenotypic plasticity and invasiveness of epithelial tumor cells. *Genes Dev.* **10,** 2462–2477 (1996).
13. Smith, A. P. *et al.* A positive role for Myc in TGFβ-induced Snail transcription and epithelial-to-mesenchymal transition. *Oncogene* **28,** 422–430 (2009).
14. Zhang, Y. E. Non-SMAD pathways in TGF-β signaling. *Cell Res.* **19,** 128–139 (2009).
15. Muraoka-Cook, R. S. *et al.* Activated type I TGFβ receptor kinase enhances the survival of mammary epithelial cells and accelerates tumor progression. *Oncogene* **25,** 3408–3423 (2006).
16. Parvani, J. G., Taylor, M. A. & Schiemann, W. P. Noncanonical TGF-β signaling during mammary tumorigenesis. *J. Mammary Gland Biol. Neoplasia* **16,** 127–146 (2011).
17. Lonn, P., Moren, A., Raja, E., Dahl, M. & Moustakas, A. Regulating the stability of TGFβ receptors and SMADs. *Cell Res.* **19,** 21–35 (2009).
18. De Boeck, M. & ten Dijke, P. Key role for ubiquitin protein modification in TGFβ signal transduction. *Ups J. Med. Sci.* **117,** 153–165 (2012).
19. Zhu, H., Kavsak, P., Abdollah, S., Wrana, J. L. & Thomsen, G. H. A SMAD ubiquitin ligase targets the BMP pathway and affects embryonic pattern formation. *Nature* **400,** 687–693 (1999).
20. Lin, X., Liang, M. & Feng, X. H. SMURF2 is a ubiquitin E3 ligase mediating proteasome-dependent degradation of SMAD2 in transforming growth factor-β signaling. *J. Biol. Chem.* **275,** 36818–36822 (2000).
21. Zhang, Y., Chang, C. B., Gehling, D. J., Hemmati-Brivanlou, A. & Delynck, R. Regulation of SMAD degradation and activity by SMURF2, an E3 ubiquitin ligase. *Proc. Natl Acad. Sci. USA* **98,** 974–979 (2001).
22. Lo, R. S. & Massague, J. Ubiquitin-dependent degradation of TGF-β-activated SMAD2. *Nat. Cell Biol.* **1,** 472–478 (1999).
23. Nijman, S. M. B. *et al.* A genomic and functional inventory of deubiquitinating enzymes. *Cell* **123,** 773–786 (2005).
24. Yuan, J., Luo, K. T., Zhang, L. Z., Cheville, J. C. & Lou, Z. K. USP10 regulates p53 localization and stability by deubiquitinating p53. *Cell* **140,** 384-U121 (2010).
25. Williams, S. A. *et al.* USP1 deubiquitinates ID proteins to preserve a mesenchymal stem cell program in osteosarcoma. *Cell* **146,** 917–929 (2011).
26. Nakada, S. *et al.* Non-canonical inhibition of DNA damage-dependent ubiquitination by OTUB1. *Nature* **466,** 941-U959 (2010).
27. Inui, M. *et al.* USP15 is a deubiquitylating enzyme for receptor-activated SMADs. *Nat. Cell Biol.* **13,** 1368-U1187 (2011).
28. Kavsak, P. *et al.* SMAD7 binds to SMURF2 to form an E3 ubiquitin ligase that targets the TGFβ receptor for degradation. *Molecular Cell.* **6,** 1365–1375 (2000).
29. Suzuki, C. *et al.* SMURF1 regulates the inhibitory activity of SMAD7 by targeting SMAD7 to the plasma membrane. *J. Biol. Chem.* **277,** 39919–39925 (2002).
30. Eichhorn, P. J. *et al.* USP15 stabilizes TGF-β receptor I and promotes oncogenesis through the activation of TGF-β signaling in glioblastoma. *Nat. Med.* **18,** 429–435 (2012).
31. Zhou, F. *et al.* Ubiquitin-specific protease 4 mitigates Toll-like/interleukin-1 receptor signaling and regulates innate immune activation. *J. Biol. Chem.* **287,** 11002–11010 (2012).
32. Guglielmo, G. M. Distinct endocytic pathways regulate TGF-β receptor signalling and turnover. *Nat. Cell Biol.* **5,** 410–421 (2003).
33. Zhang, X. N., Berger, F. G., Yang, J. H. & Lu, X. B. USP4 inhibits p53 through deubiquitinating and stabilizing ARF-BP1. *EMBO J.* **30,** 2177–2189 (2011).
34. Xu, J., Lamouille, S. & Derynck, R. TGF-β-induced epithelial to mesenchymal transition. *Cell Res.* **19,** 156–172 (2009).
35. Thiery, J. P., Acloque, H., Huang, R. Y. & Nieto, M. A. Epithelial-mesenchymal transitions in development and disease. *Cell* **139,** 871–890 (2009).
36. He, S. *et al.* Neutrophil-mediated experimental metastasis is enhanced by VEGFR inhibition in a zebrafish xenograft model. *J. Pathol.* http://dx.doi.org/10.1002/path.4013 (2012).
37. Kang, Y. B. *et al.* A multigenic program mediating breast cancer metastasis to bone. *Cancer Cell* **3,** 537–549 (2003).
38. Bandyopadhyay, A. *et al.* Inhibition of pulmonary and skeletal metastasis by a transforming growth factor-β type I receptor kinase inhibitor. *Cancer Res.* **66,** 6714–6721 (2006).
39. Manning, B. D. & Cantley, L. C. AKT/PKB signaling: navigating downstream. *Cell* **129,** 1261–1274 (2007).
40. Tran, H., Brunet, A., Griffith, E. C. & Greenberg, M. E. The many forks in FOXO's road. Sci STKE **2003**, RE5 (2003).
41. Freeman, A. K. & Morrison, D. K. 14-3-3 Proteins: diverse functions in cell proliferation and cancer progression. *Semin. Cell Dev. Biol.* **22,** 681–687 (2011).
42. Wada, K. & Kamitani, T. UnpEL/Usp4 is ubiquitinated by Ro52 and deubiquitinated by itself. *Biochem. Biophys. Res. Commun.* **342,** 253–258 (2006).
43. Sowa, M. E., Bennett, E. J., Gygi, S. P. & Harper, J. W. Defining the human deubiquitinating enzyme interaction landscape. *Cell* **138,** 389–403 (2009).
44. Fan, Y. H. *et al.* USP4 targets TAK1 to downregulate TNFα-induced NF-κB activation. *Cell Death Differ.* **18,** 1547–1560 (2011).
45. Xiao, N. *et al.* Ubiquitin-specific protease 4 (USP4) targets TRAF2 and TRAF6 for deubiquitination and inhibits TNF α-induced cancer cell migration. *Biochem. J.* **441,** 979–986 (2012).
46. Inui, M. *et al.* USP15 is a deubiquitylating enzyme for receptor-activated SMADs. *Nat. Cell Biol.* **13,** 1368–1375 (2011).
47. Conery, A. R. *et al.* AKT interacts directly with SMAD3 to regulate the sensitivity to TGF-β-induced apoptosis. *Nat. Cell Biol.* **6,** 366–372 (2004).
48. Remy, I., Montmarquette, A. & Michnick, S. W. PKB/AKT modulates TGF-β signalling through a direct interaction with SMAD3. *Nat. Cell Biol.* **6,** 358–365 (2004).
49. Daly, A. C., Vizan, P. & Hill, C. S. SMAD3 protein levels are modulated by Ras activity and during the cell cycle to dictate transforming growth factor-β responses. *J. Biol. Chem.* **285,** 6489–6497 (2009).
50. Han, S. U. *et al.* Loss of the SMAD3 expression increases susceptibility to tumorigenicity in human gastric cancer. *Oncogene* **23,** 1333–1341 (2004).
51. Cohen, P. & Tcherpakov, M. Will the ubiquitin system furnish as many drug targets as protein kinases? *Cell* **143,** 686–693 (2010).

METHODS

Cell culture and reagents. MEFs from wt and USP4-deficient mice were provided by X. Lu (University of Texas MD Anderson Cancer Center, Houston, Texas, USA). HEK293T cells, HeLa cervical cancer cells, MDA-MB-231 breast cancer cells and MEFs were cultured in Dulbecco's modified Eagle's medium with 10% FBS and 100 U ml^{-1} penicillin–streptomycin. Myc–USP4 wt and Myc–USP4^{CS} expression constructs were cloned and verified by DNA sequencing. USP4 wt and USP4^{CS} were subcloned into the pLV bc puro lentivirus construct. USP4^{S445A} and USP4^{S445D} were made by site-directed mutagenesis and confirmed by DNA sequencing. Myr-AKT1 constructs were kindly provided by P. Coffer (University Medical Center Utrecht, The Netherlands). Reagents used were MG132 (Sigma), IGF-1 (R&D 291-G1), LY294002 (Cell Signaling) and λ-phosphatase (Biolabs). The antibodies used for immunoprecipitation (IP), immunoblotting (IB) and immunofluorescence: β-actin 1:10,000 (IB; A5441, Sigma), c-Myc 1:1,000 (IB; a-14, sc-789, Santa Cruz Biotechnology), HA 1:1,000 (IB; Y-11, sc-805, Santa Cruz Biotechnology), HA 1:10,000 (IB; 12CA5, home-made), Flag 1:10,000 (IB; M2, Sigma), USP4 1:2,000 (IB); 1:200 (IP; U0635, Sigma), TβRI 1:1,000 (IB); 1:100 (IP; V22, Santa Cruz), AKT 1:5,000 (IB); 1:250 (IP; no. 2938, Cell Signaling), phosphor-AKT substrate (RXRXXS*-T*) 1:1,000 (IB; no. 10001, Cell Signaling), phosphor-AKT (Ser 473) 1:1,000 (IB; no. 9271, Cell Signaling), V5 1:5,000 (IB; Invitrogen), USP15 1:5,000 (IB); 1:200 (IP; BETHYL), USP11 1:5,000 (IB; BETHYL A301-613A), USP19 1:2,500 (IB; BETHYL A301-586A), N-cadherin 1:10,000 (IB; 610920, BD), tubulin 1:1,000 (IB; no. 2146, Cell Signaling), HDAC3 1:1,000 (IB; no. 3949, Cell Signaling), SMAD4 1:1,000 (IB; B8, Santa Cruz), SMAD2-3 1:2,500 (IB); 1:500 (IP; 610842 BD), phospho-SMAD2 1:5,000 (IB; no. 3101, Cell Signaling), Ub 1:1,000 (IB; P4D1 Santa Cruz), fibronectin 1:1,000 (IB; Sigma), SMA (Sigma), vimentin 1:1,000 (IB; no. 5741 Cell Signaling) and E-cadherin 1:10,000 (IB; BD 610181). Recombinant proteins used were human active AKT1 protein (R&D, 1775-KS), TGFβR1(ALK5) active (SignalChem, T07-11G) and GST–TGFβR1-ICD (ProQinase, 0397-0000-1).

cDNA screen. HEK293T cells stably transfected with SMAD3–SMAD4-dependent $CAGAR_{12}$–Luc transcriptional reporter were used as a readout system to identify regulators of TGF-β signalling. We first set the stimulation using a suboptimal dose, 0.075 ng ml^{-1} of TGF-β1 to get about 30% of the highest stimulation level (2 ng ml^{-1} of TGF-β 1), so we could look for both activators and inhibitors. Both the Origene10K (2 sets) and MGC7K cDNA libraries[52] (total 27,000 genes) were screened in duplicate with a control plate containing pCMV–SPORT6, CMV–SMAD7 and CMV–SMAD3. cDNAs were cherry picked, transformed and plasmid DNAs purified. Each cDNA was then re-screened in duplicate. Sixty-nine Flag-tagged human DUBs cDNA were re-screened in triplicate. Similar expression of each DUB was checked by western blot analysis. The screen data are available in PubChem BioAssay through the link: http://pubchem.ncbi.nlm.nih.gov/assay/assay.cgi?aid=624128.

Lentiviral transduction and generation of stable cell lines. Lentiviruses were produced by transfecting shRNA-targeting plasmids together with helper plasmids pCMV–VSVG, pMDLg–RRE (gag–pol), and pRSV–REV into HEK293T cells. Cell supernatants were collected 48 h after transfection and were either used to infect cells or stored at −80 °C.

To obtain stable cell lines, cells were infected at low confluence (20%) for 24 h with lentiviral supernatants diluted 1:1 with normal culture media in the presence of 5 ng ml^{-1} of Polybrene (Sigma). Cells were subjected to under puromycin selection 48 h after infection for one week and then passaged before use. Puromycin was used at 1 μg ml^{-1} to maintain MDA-MB-231 cells. Lentiviral shRNAs were obtained from Sigma (MISSION shRNA). Typically, 5 shRNAs were identified and tested, and the most effective two shRNAs were used for the experiment. We used TRCN0000004040 (no. 1), 5′-CCGGCCCAACTGTAAGAAGCATCAACTCGAGTTGATGCTTCTTACAGTTG-GGTTTTT-3′, TRCN0000004041 (no. 2), 5′-CCGGGCCCAGAATGTGCTAAG-GTTTCTCGAGAAACCTTAGCACATTCTGGGCTTTTT-3′ and 5′-TRCN00000-04042-3′ (no. 3), 5′-CCGGGAGGCGTGGAATAAACTACTACTCGAGTAGTAG-TTTATTCCACGCCTCTTTTT-3′ for human USP4 knockdown.

Immunoprecipitation, immunoblotting and biotinylation. Cells were lysed with 1 ml lysis buffer (20 mM Tris–HCl at pH 7.4, 2 mM EDTA, 25 mM NaF and 1% Triton X-100) plus protease inhibitors (Sigma) for 10 min at 4 °C. After centrifugation at $12 \times 10^3 \times g$ for 15 min, the protein concentration was measured, and equal amounts of lysate were used for immunoprecipitation. Immunoprecipitation was performed with different antibodies and protein A–Sepharose (GE Healthcare Bio-Sciences AB) for 3 h at 4 °C. Thereafter, the precipitants were washed three times with washing buffer (50 mM Tris–HCl at pH 8.0, 150 mM NaCl, 1% Nonidet P-40, 0.5% sodium deoxycholate and 0.1% SDS) and the immune complexes eluted with sample buffer containing 1% SDS for 5 min at 95 °C. The immunoprecipitated proteins were then separated by SDS–PAGE. Western blotting was performed with specific antibodies and secondary anti-mouse or anti-rabbit antibodies conjugated to horseradish peroxidase (Amersham Biosciences). Visualization was achieved with chemiluminescence detection. For proteins that were close to the IgG heavy chain, for example, TβRI blots, the protein A–HRP was used. For biotinylation analysis of cell surface receptors, the cells were biotinylated for 40 min at 4 °C and then incubated at 37 °C for the indicated times. The biotinylated cell surface receptors were precipitated with streptavidin beads and analysed by immunoblotting.

Purification of bacterially expressed recombinant USP4 proteins. GST–USP4 wt and mutant expression constructs were generated by sub-cloning into pGEX-4T1 vectors. GST–USP4 plasmids were used to transform the *Escherichia coli* strain BL21 or Rosetta, respectively. Cultures were grown overnight at 37 °C. The next day, cultures were diluted 1:50 in fresh LB medium and grown at 37 °C to an attenuance of 0.6 at 600 nm. Cells were then induced overnight at 24 °C in the presence of 0.5 mM isopropyl-β-D-thiogalactopyranoside (IPTG), 20 mM HEPES at pH 7.5, 1 mM $MgCl_2$ and 0.05 % glucose. For GST–USP4 purification, the washed pellets were resuspended in lysis buffer (PBS, 0.5 M NaCl, complete protease inhibitors (Roche), 1 mM phenylmethyl sulphonyl fluoride and 1% Triton X-100). After sonication and a freeze–thaw step, the supernatants of the cell lysates were incubated with glutathione Sepharose (GE Healthcare). Beads were washed twice with lysis buffer and three times with 50 mM Tris at pH 7.5 and 0.5 M NaCl. Purified proteins were eluted in 50 mM Tris at pH 7.5, 0.5 M NaCl and 20 mM glutathione. For purification of USP4 protein, GST was removed by biotin-tagged thrombin.

***In vitro* deubiquitylation of TβRI.** Poly-HA-ubiquitylated TβRI–Flag substrates were prepared by transiently co-transfecting HEK293T cells with TβRI–Flag and HA–ubiquitin. Thirty-six hours later, cells were treated with MG132 (5 μM) for 4 h and then the poly-HA-ubiquitylated TβRI–Flag was purified in denaturing conditions. To assay the ability of the USP4 protein to deubiquitylate TβRI *in vitro*, recombinant USP4 protein was incubated with purified poly-HA-ubiquitylated TβRI at 37 °C for 1 h. Reactions were terminated by SDS sample buffer followed by a 2 min heat denaturation at 95 ○C. Reaction products were detected by western blot analysis.

Zebrafish embryo analysis. Zebrafish (*Danio rerio*), AB strain, were kept at 28.5 °C under a light and dark cycle of 14 and 10 h, respectively. Fish staging and embryo production were carried out as described previously[53,54]. Capped mRNAs were synthesized using T7 Cap Scribe (Roche) according to the manufacturer's instructions. For preparation of the digoxigenin-labelled antisense probe, plasmid containing the USP4 cDNAs was linearized with KpnI. Linearized template DNA was transcribed *in vitro* with T7 polymerase using digoxigenin–UTP (Roche). *In situ* hybridizations were performed as previously described[55]. Embryo stages are given in hpf at standard temperature.

To knockdown USP4 gene function, morpholino oligonucleotides were synthesized by Gene Tools company (*zusp* 4-MO: 5′-AGCGAGTGAACCCGCAGTGACC-GCG-3′). The control morpholino sequence was 5′-GCGCCATTGCTTTGCAAGA-ATTG-3′. All oligonucleotides were dissolved in nuclease-free water to make a 24-μg per μl storage concentration. The mRNAs and morpholino oligonucleotides were injected into the yolk of fertilized eggs at the single-cell stage. All of the embryo injections were carefully controlled with the same amount of control morpholino and control GFP mRNA.

Total RNA was isolated from embryos at different stages using Trizol reagent (TAKARA). The first-strand cDNAs synthesized from total RNAs were used as templates following the SuperScript Kit (Invitrogen). qRT-PCR reactions were performed for 30 cycles and a final extension for 6 min with an internal β-actin control. The primers used are listed in Supplementary Table S2.

Migration and invasion assays. Transwell assays were performed in 24-well polyethylene terephthalate inserts (Falcon, 8.0- μm pore size) for migration assays. MDA-MB-231 stable cells were serum starved overnight. Then, 50×10^3 or 10×10^3 cells were plated in Transwell inserts (at least three replicas for each sample) and left treated with or without SB431542 (5 μM) for 8 h. Cells in the upper part of the Transwells were removed with a cotton swab; migrated cells were fixed in 4% paraformaldehyde and stained with crystal violet 0.5%. Filters were photographed in 4 random fields and the number of cells counted. Every experiment was repeated independently at least three times.

Zebrafish embryonic invasion and metastasis assay. We used a zebrafish embryo xenograft model described previously[36], where mammalian tumour cells are injected into the zebrafish embryonic blood circulation. Approximately 400 tumour cells labelled with a red fluorescent cell tracer were injected into the blood of 48-hpf *fli-casper* zebrafish embryos at the ducts of Cuvier[56] (Fig. 3d). After injection, some

DOI: 10.1038/ncb2522

of the tumour cells disseminated into the embryo blood circulation whereas the rest remained in the yolk. Zebrafish embryos were maintained for 5 dpi at 33 °C, a compromise for both the fish and the cell lines[57]. The tumour cells that enter into the blood stream preferentially invaded and micrometastasized into the posterior tail fin area (Fig. 3e). Invasion could be visualized as a single cell that has left the blood vessel, which can subsequently form a micrometastasis (3–50 cells). Pictures were taken by confocal microscopy at 1, 3 and 5 dpi, and the percentages of invasion and micrometastasis were counted. Every experiment was repeated at least two times independently.

Statistical analysis. Statistical analyses were performed with a two-tailed unpaired *t*-test. $P < 0.05$ was considered statistically significant.

Transcription reporter assay, immunofluorescence microscopy, ubiquitylation assays, nickel pulldown assays, qRT-PCR and cellular fractions. These experiments were carried out as previously described[31,58,59]. All of the primers used for qRT-PCR are listed in Supplementary Table S2.

52. Strausberg, R. L., Feingold, E. A., Klausner, R. D. & Collins, F. S. The mammalian gene collection. *Science* **286,** 455–457 (1999).
53. Cao, Y., Zhao, J., Sun, Z. H., Postlethwait, J. & Meng, A. M. fgf17b, a novel member of Fgf family, helps patterning zebrafish embryos. *Dev. Biol.* **271,** 130–143 (2004).
54. Zhang, L. X. *et al.* Zebrafish Dpr2 inhibits mesoderm induction by promoting degradation of nodal receptors. *Science* **306,** 114–117 (2004).
55. Prince, V. E., Price, A. L. & Ho, R. K. Hox gene expression reveals regionalization along the anteroposterior axis of the zebrafish notochord. *Dev. Genes Evol.* **208,** 517–522 (1998).
56. White, R. M. *et al.* Transparent adult zebrafish as a tool for *in vivo* transplantation analysis. *Cell Stem Cell* **2,** 183–189 (2008).
57. Lee, L. M. J., Seftor, E. A., Bonde, G., Cornell, R. A. & Hendrix, M. J. C. The fate of human malignant melanoma cells transplanted into zebrafish embryos: assessment of migration and cell division in the absence of tumor formation. *Dev. Dynam.* **233,** 1560–1570 (2005).
58. Nakao, A. *et al.* Identification of SMAD7, a TGFβ-inducible antagonist of TGF-β signalling. *Nature* **389,** 631–635 (1997).
59. Zhang, L. *et al.* Fas-associated factor 1 antagonizes Wnt signaling by promoting beta-catenin degradation. *Mol. Biol. Cell* **22,** 1617–1624 (2011).

DOI: 10.1038/ncb2522

nature cell biology

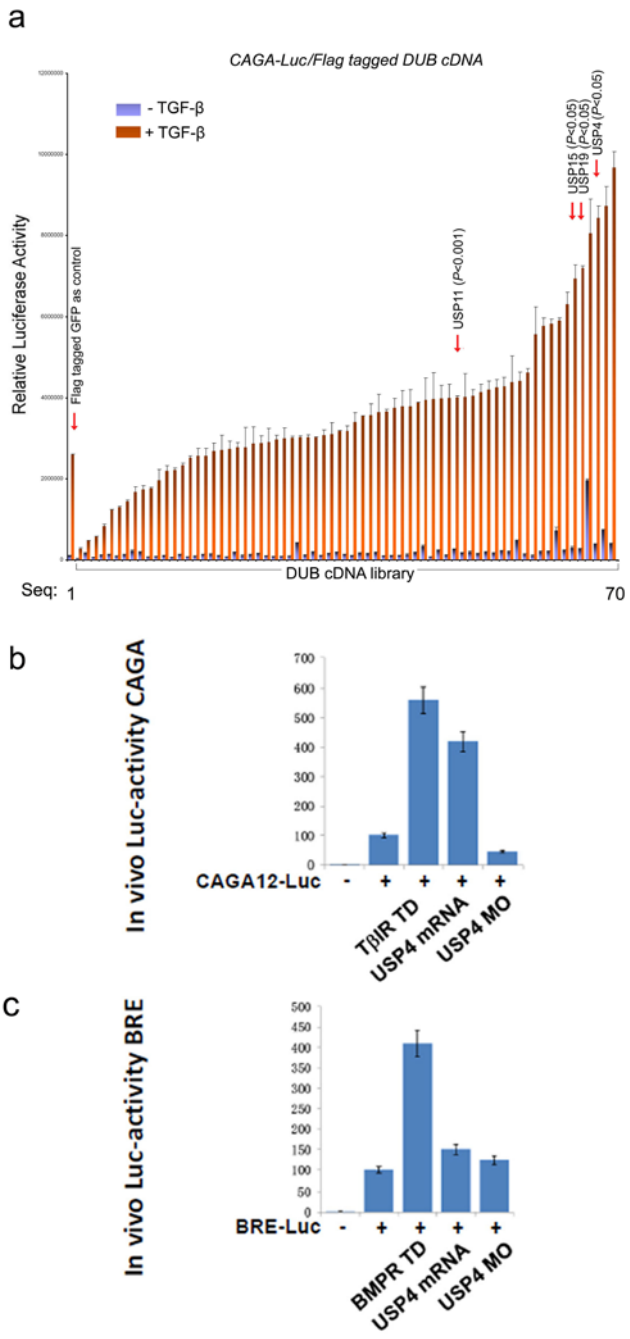

Figure S1 DUB cDNA overexpression screen identified USP4 and other DUBs (USP15, USP19 and to a lesser extend USP11) as potent activators of TGF-β signaling. (**a**) Graph show ligand-mediated inductions of TGF-β-induced $CAGA_{12}$-Luc transcriptional reporter activity compared to control cells and the effects of a representative set of DUB cDNAs. n=3. Numeric output of this screen was deposited in PubChem Bioassay database and available through link: http://pubchem.ncbi.nlm.nih.gov/assay/assay.cgi?aid=624128. (**b**, **c**) Effect of USP4 misexpression on TGF-β and BMP signaling activity in zebrafish embryos. CAGA-Luc (**b**) or BRE-Luc (**c**) reporter and *renilla* internal control plasmids were co-injected with *usp4* mRNA or MO to zebrafish embryos at single-cell stage. Constitutively active mutants TβRI-TD and BMPRI-TD were included as positive control. The injection values of DNA were adjusted to 100 pg per embryos. All embryos were harvested at bud stage equal to 10 h post fertilization (hpf).

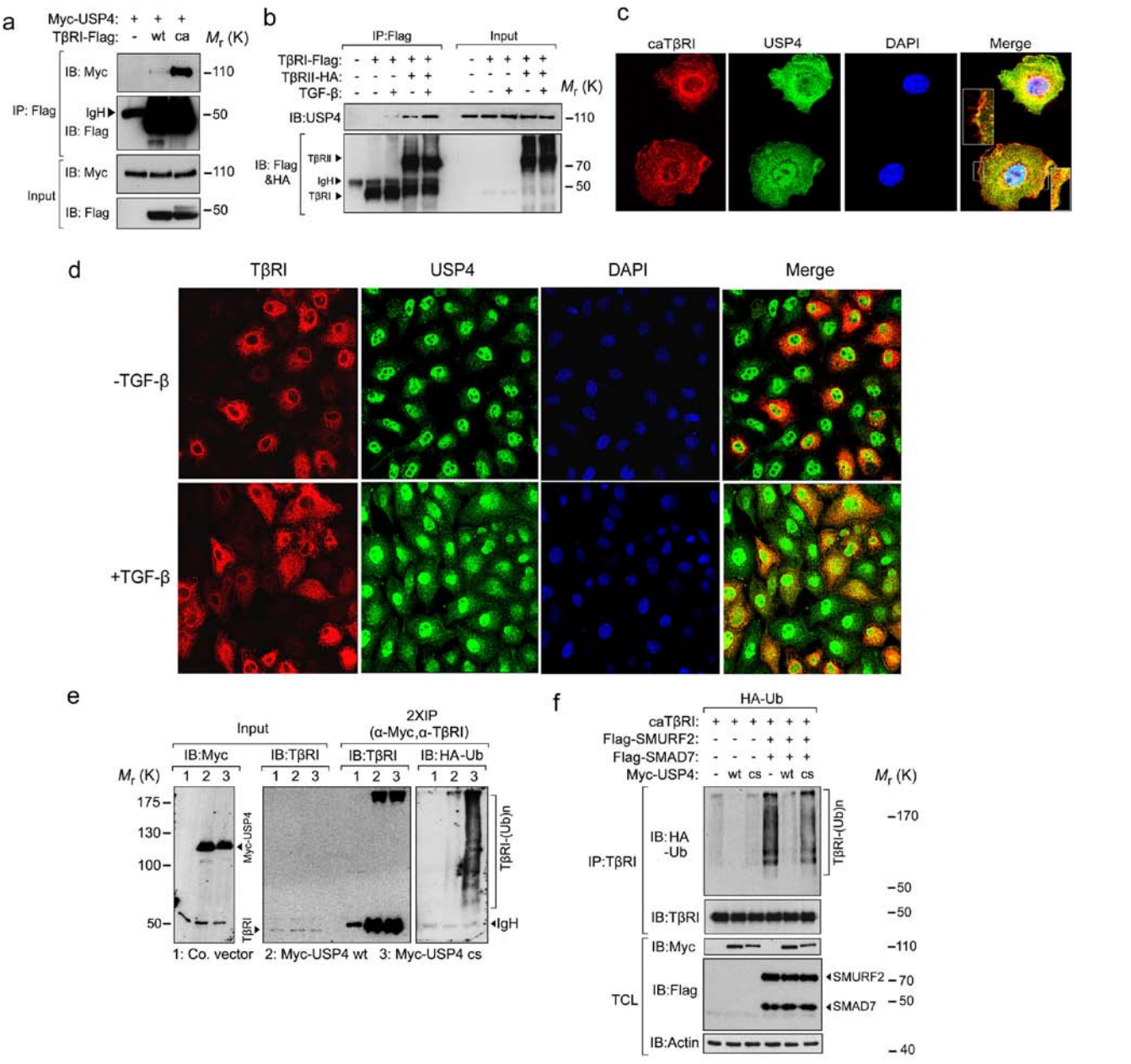

Figure S2 USP4 interacts with and deubiquitinates TβRI. (**a**) Constitutively active (ca) TβRI interacts with USP4 when overexpressed in HEK293T cells. Immunoblotting (IB) analysis of immunoprecipitates derived from HEK293T cells transfected with indicated plasmids. 5% whole cell lysates were loaded as input. (**b**) TGF-β stimulates the interaction between transfected TGF-β receptors and endogenous USP4. Immunoprecipitation (IP) and IB analysis of HeLa cells transfected with TβRI-Flag, TβRII-HA receptor and treated with TGF-β (5 ng ml^{-1}) for 4 h as indicated. (**c**) Immunofluorescence analysis and 4, 6-diamidino-2-phenylindole (DAPI) staining of HeLa cells stably transfected with Flag-tagged caTβRI and Myc-tagged USP4. Inserts are shown in the merge picture that represents higher magnifications of the plasmamembrane regions. (**d**) Immunofluorescence analysis and DAPI staining of HeLa cells stably expressing Flag-tagged TβRI (at low levels that correspond to endogenous TβRI expression level) in the absence or presence of TGF-β. Cells were stimulated for 4 h with TGF-β (5ng ml^{-1}). Localization of TβRI and USP4 were determined with anti-Flag and USP4 antibodies, respectively. (**e**) USP4 but not USP4 cs mutant potently inhibits TβRI ubiquitination. HEK293T cells transfected with control vector (Co.vector), Myc-USP4 wild-type (wt) or Myc-USP4 C311S (CS) as indicated were harvested for the first IP with anti-Myc antibody, immunoprecipitates were eluted with 2% SDS, and then diluted with RIPA buffer (to SDS concentration <0.1%), the second IP was performed with anti-TβRI antibody followed with IB analysis. Left panel: 3% cell lyses were loaded as input showing Myc-USP4 level. Middle panel: IB analysis of total TβRI and USP4-associated TβRI. Right panel: IB analysis of polyubiquitin conjungated to USP4 CS-associated TβRI. (**f**) USP4 wt, but not USP4 CS, potently antagonizes SMAD7-SMURF2-mediated poly-ubiquitination of TβRI. HA-Ub-expressed HEK293T cells were transfected with caTβRI, Flag-SMURF2, Flag-SMAD7 and Myc-USP4 wt or USP4 CS as indicated. Cells were then harvested for IP with anti-TβRI antibody followed with IB analysis for HA-Ub, TβRI, myc-USP4, Flag-SMURF2 and Flag-SMAD7.

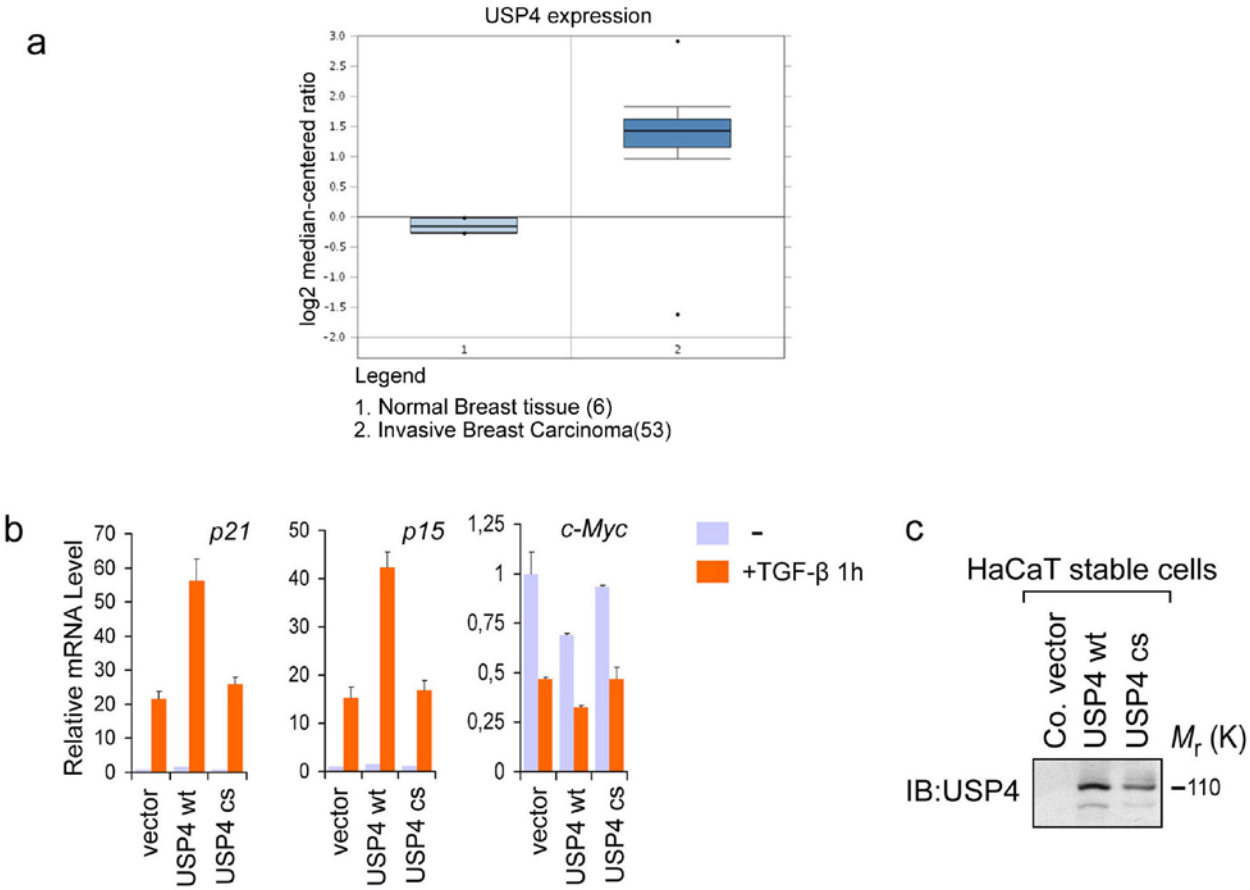

Figure S3 Breast carcinoma exhibits higher expression of USP4 and ectopic expression of USP4 in HaCaT cells amplifies TGF-β-induced cytostatic effect. (**a**) USP4 expression is higher in invasive breast carcinomas than normal breast tissues. (**b**) HaCaT stable cells expressing control vector or USP4 wt or USP4 CS were treated with or without TGF-β (5 ng ml^{-1}) for 1 h and cells were then harvested for qRT-PCR analysis for TGF-β target genes. Analysis of *p21*, *p15* and *c-Myc* gene expression is shown. (**c**) HaCaT stable cell lines transfected with control vector or USP4 wt or USP4 CS expression vector. The same amount of cell lysates from HaCaT stable cells were subjected to immunoblot analysis with USP4 antibodies.

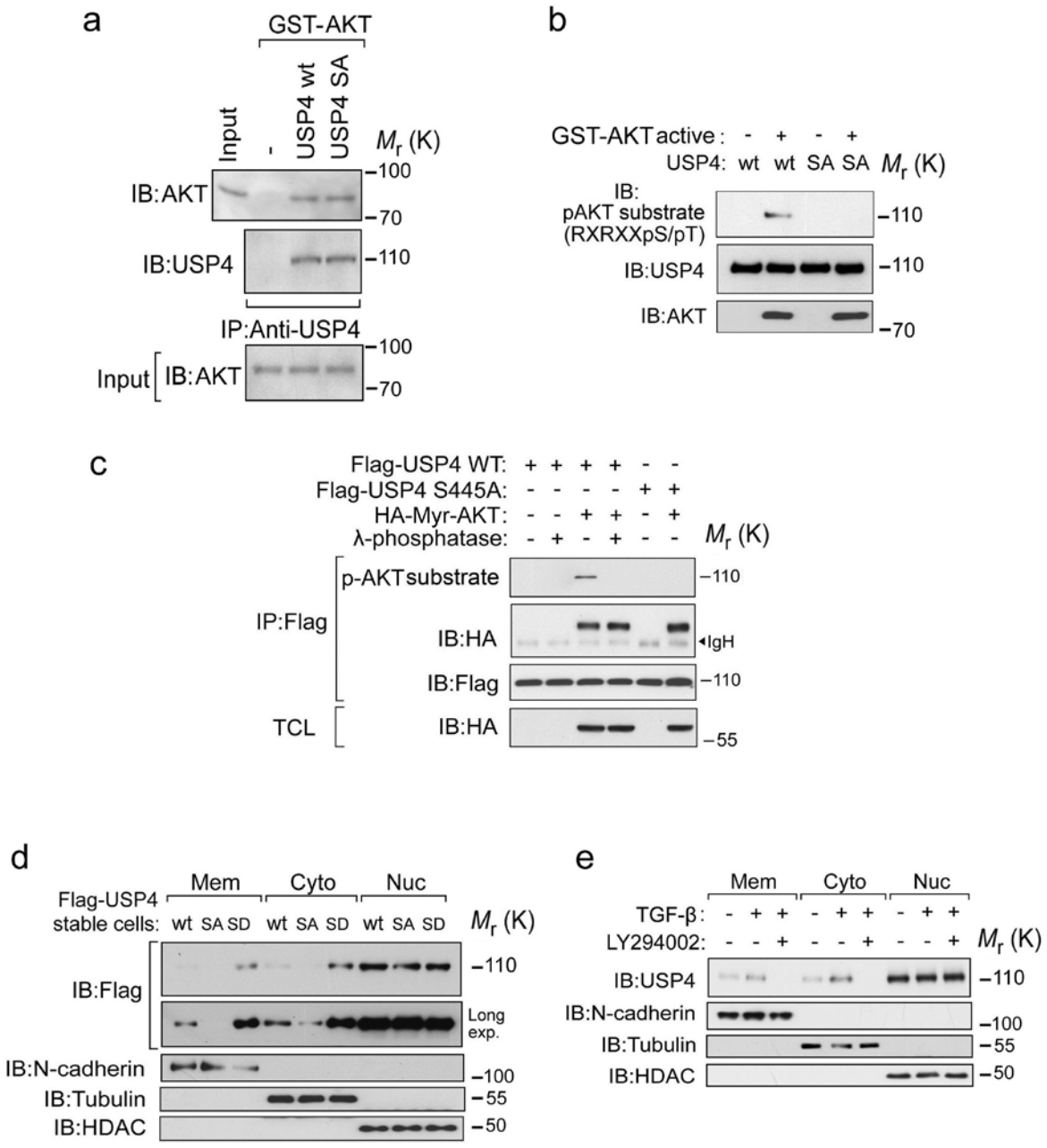

Figure S4 AKT phosphorylates USP4. (**a**) Interaction of purified USP4 wt and USP4 S445A with GST-AKT *in vitro*. (**b**) *In vitro* phosphorylation assay of bacterially expressed purified USP4 wt and AKT-phospho site mutant (S455A) by purified human active GST-AKT fusion protein. Direct USP4 phosphorylation by AKT was determined by immunoblot (IB) analysis with p-AKT substrate (RXRXXpS(pT)) phospho antibodies. USP4 and AKT were included as loading controls. (**c**) USP4, but not USP4 S445A, is phosphorylated by activated AKT. Immunoprecipitation (IP) and IB analysis of HEK293T cells transfected with Flag-USP4 WT, Flag-USP4 S445A and HA-Myr-AKT and preincubated with or without λ-phosphatase as indicated. (**d**) USP4 wt and USP4 S455D, but not USP4 S455A, exist in membrane and cytosol fractions. HeLa cells transfected with USP4 wt, USP4-S445A, and HA-Myr-AKT as indicated were harvested for membrane, cytoplasm, and nuclear extraction and followed by IB analysis. (**e**) TGF-β stimulates membrane and cytosol localization of USP4, whereas co-treatment with PI3K inhibitor LY294002 inhibits this TGF-β-induced response. HeLa cells were treated with TGF-β (5 ng ml^{-1}) and LY294002 (50 μM) for 8 h as indicated. Cells were then harvested for membrane, cytoplasm, and nuclear extraction and followed by IB analysis. For **d, e**, N-cadherin, tubulin, and histone deacetylase (HDAC)3 were analyzed as the membrane (mem), cytoplasm (cyto), and nuclear (nuc) fraction markers, respectively.

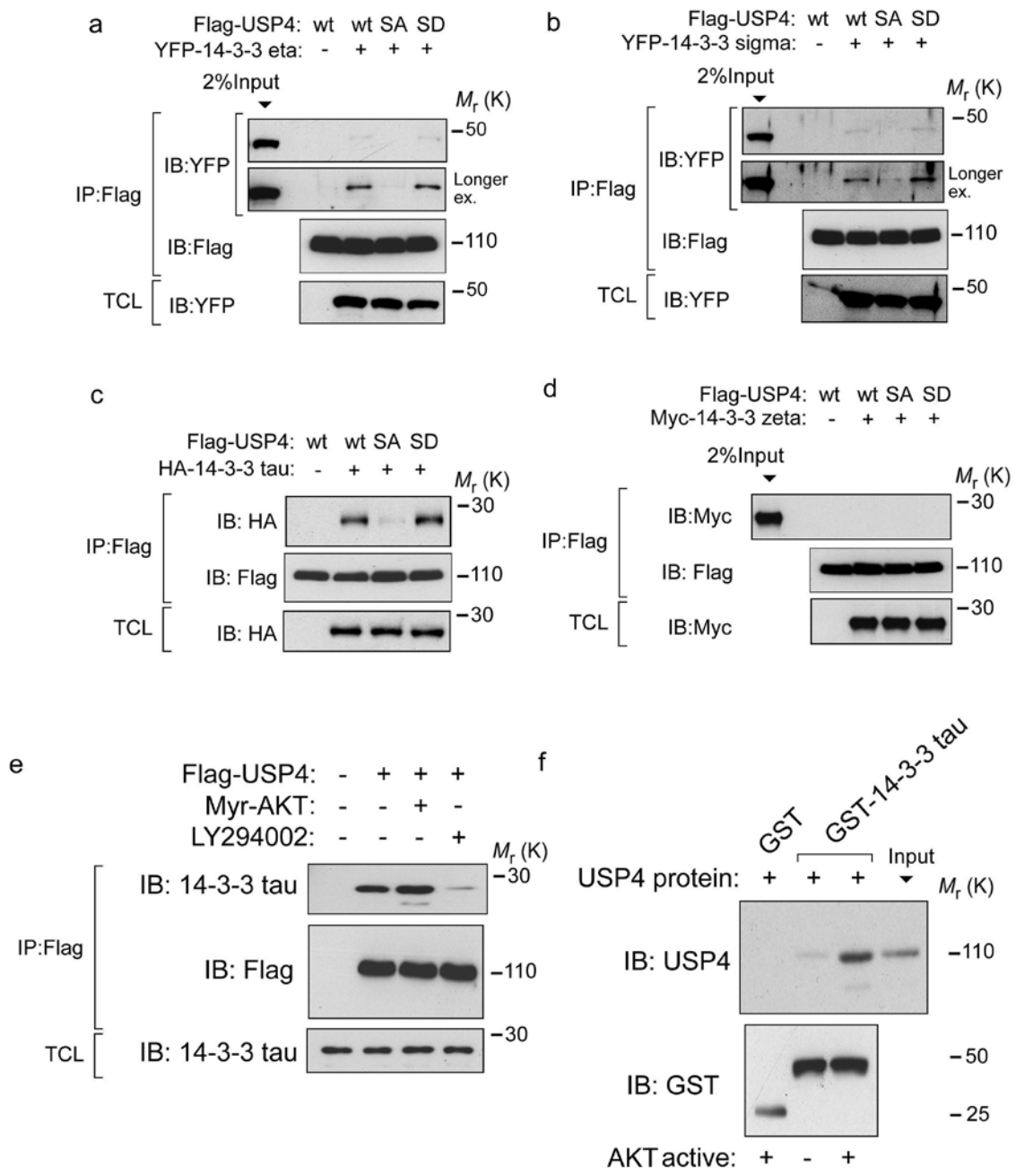

Figure S5 14-3-3 eta/sigma/tau, but not 14-3-3 zeta binds to AKT-phosphorylated USP4. **(a-d)** Immunoblot (IB) analysis of whole cell lysate (TCL) and immunoprecipitates derived from HEK293T cells transfected with Flag-USP4 wt, USP4-S455A, or USP4-S455D and YFP-14-3-3 eta (**a**) YFP-14-3-3 sigma (**b**) HA-14-3-3 tau (**c**) Myc-14-3-3 zeta (**d**). The results in (**a-d**) show that compared with USP4 wt and USP4 S445D, USP4 S445A lost its ability to associate with 14-3-3. (**e**) Myr-AKT promotes and LY294002 treatment suppresses the interaction between Flag-USP4 and endogenous 14-3-3 tau. 293T cells transfected as indicated were treated with LY294002 (50 μM) for 8 h, and harvested for co-immunoprecipitation experiments and IB analysis. (**f**) 14-3-3 tau directly interacts with USP4 *in vitro,* when USP4 is pretreated with active AKT.14-3-3 tau bound to glutathione-agarose beads were incubated *in vitro* with USP4 protein, which was pre-incubated for 30 min with recombinant active AKT kinase at 30 °C. Samples were washed and subsequently subjected to IB analysis.

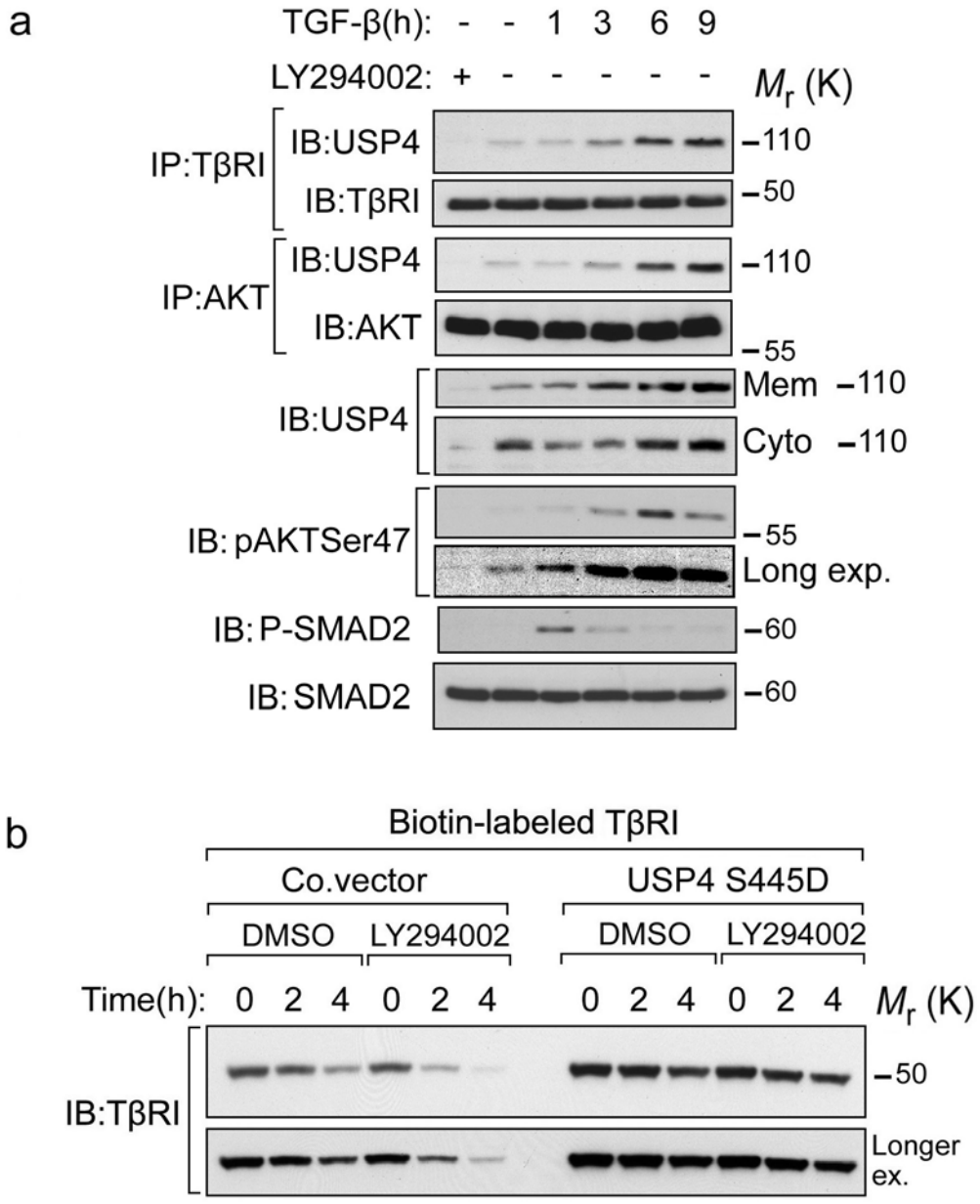

Figure S6 Activation of AKT-USP4 is required for TβRI stabilization. (**a**) HeLa cells were treated with LY294002 (50 μM) or TGF-β (5 ng ml^{-1}) with indicated time points. Cells were harvested for anti-TβRI and anti-AKT immunoprecipitations and then blotted with anti-USP4. Total cell lysates were immunoblotted (IB) with p-SMAD2, total SMAD2 and pAKT Ser473, as indicated. Membrane (Mem) and cytosolic (Cyto) fractions were separated and analyzed for USP4 levels by IB analysis with USP4 antibodies. (**b**) HeLa cells stably expressing control vector or USP4 S445D were treated with DMSO or LY294002 (50 μM) for 6 h, the membranre proteins were biotinlabeled and then incubated at 37 °C for 2 or 4 h as indicated. Biotinylated cell surface receptors were precipitated with streptavidin beads and analyzed by anti-TβRI immunoblot.

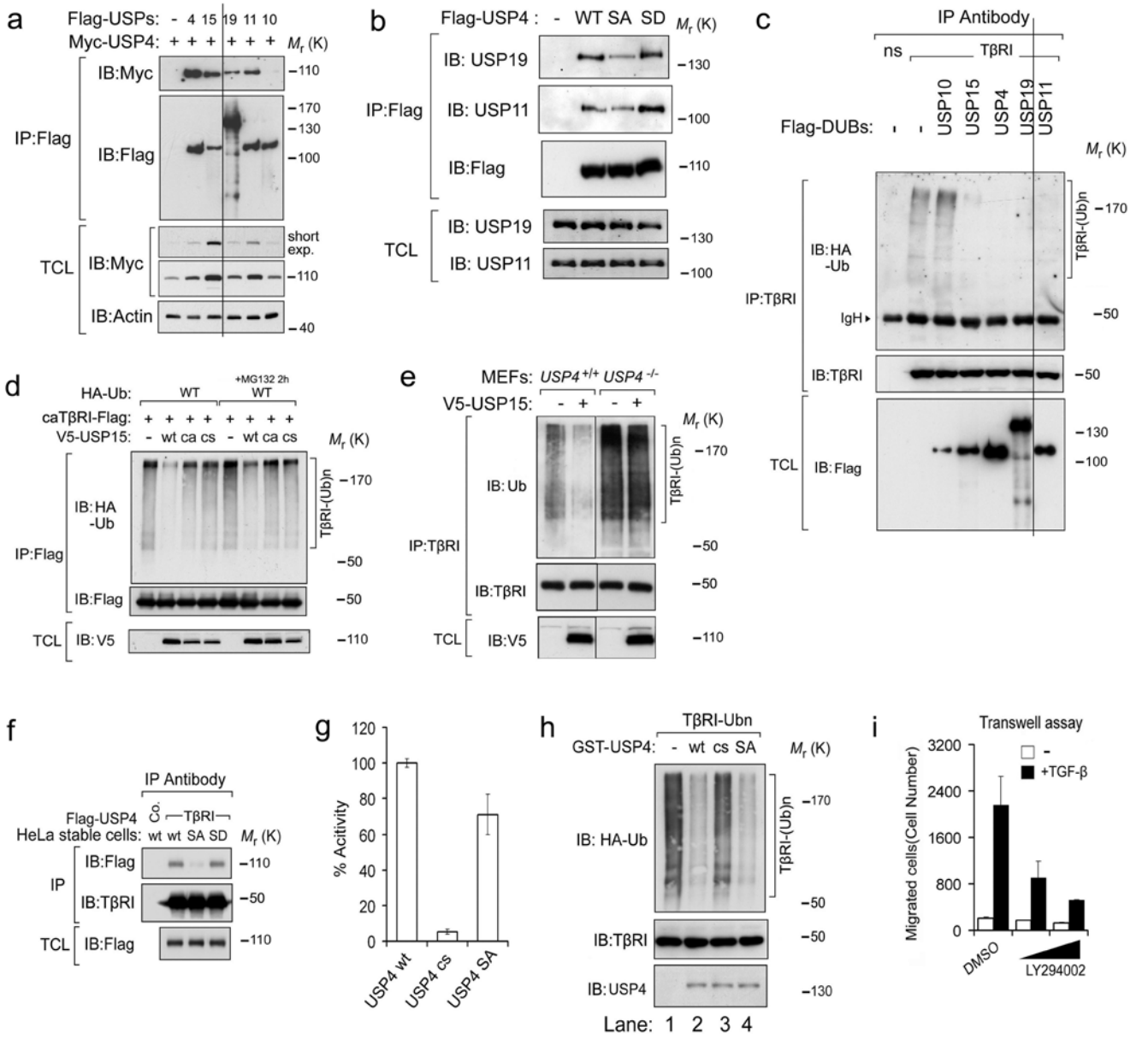

Figure S7 Functional DUBs in regulating TβRI ubiquitination. (**a**) USP4 interacts with itself and with USP11, 15 and 19 when coexpressed in HEK 293 cells. Immunoblotting (IB) analysis of whole cell lysate (TCL) and immunoprecipitates derived from HEK293T cells transfected with Myc-USP4 along with Flag-USPs. USP10 was employed as a negative control. (**b**) USP4 WT and SD mutant interact more efficiently with USP11 and 19 than USP4 S455A mutant. IB analysis of whole cell lysate (TCL) and immunoprecipitates derived from HEK293T cells transfected with Flag-USP4 wt, USP4 S445A (SA) or USP4 S445D (SD). (**c**) USP4, 11, 15 and 19 (but not USP10) inhibit TβRI ubiquitination. HA-Ub-expressed HEK293T cells were transfected with Flag-DUBs as indicated. Cells were then treated with MG132 (5 μM) for 4 h and harvest for immunoprecipitation (IP) and IB analysis. (**d**) USP15 wt, but not the DUB inactive mutants, inhibits TβRI ubiquitination. IB analysis of whole cell lysate (TCL) and immunoprecipitates derived from HA-Ub-expressed HEK293T cells transfected with caTβRI-Flag or V5-USP15 wt or USP15 C269A (CA) or USP15 C269S (CS) and with or without MG132 (5 μM) treatment. (**e**) USP15 deubiquitination of TβRI is dependent on USP4 expression. IB analysis of whole cell lysate (TCL) and immunoprecipitates derived from *USP4* wt and *USP4* deficient MEFs transfected with or without V5-USP15. (**f**) Hydrolysis of the ubiquitin-AMC substrate by the USP4 wt, USP4 CS or USP4 S455A. The data are shown as mean ± SD. n=5. Recombinant USP4 proteins were incubated for 30 min at 37 °C in 200 μl of 0.5 μM ubiquitin-AMC. The fluorescence was determined at an excitation wavelength of 380 nm and an emission of 460 nm. Less than 5% of the substrate was cleaved during the incubation (not shown). (**g**) Poly-HA-ubiquitinated TβRI substrate (purified in denatured condition) was incubated with purified recombinant USP4 wt, USP4 CS or USP4 S455A at 37 °C for 1 h. Reaction was terminated by addition of SDS sample buffer followed by a 2 min heat denaturation at 95 °C. Reaction products were detected by IB analysis using indicated antibodies. Note those lanes 1-3 were also shown as Fig. 2e. (**h**) Membrane fraction of Flag-USP4 wt, USP4 S455A (SA) or USP4 S455D (SD) stably expressed HeLa cells were subjected to anti-TβRI immunoprecipitation and anti-Flag IB analysis. (**i**) MDA-MB231 cells were plated for cell migration assays. Cells were treated with combination of TGF-β (5 ng ml^{-1}) and LY294002 (25 or 50 μM) for 8 h. Migrated cells were counted from four random fields, and mean ± SD were calculated (P<0.05).